Research Square

Preprints are preliminary reports that have not undergone peer review.
They should not be considered conclusive, used to inform clinical practice,
or referenced by the media as validated information.

Potato Peel Extract as an ecologically conscious Inhibitor for corrosion of A283 Carbon Steel in Hydrochloric Acid: Experimental and Theoretical Perspectives

Metwally Abdallah

metwally555@yahoo.com

Benha University

Omar A. Hazazi

Umm Al-Qura University

Dina Walid

Benha University

Salih S. Al-Juaid

King Abdulaziz University

Doaa F. Seyam Seyam

Benha University

Ali Y. El-Etre

Benha University

Elsayed M. Mabrouk

Benha University

Nahed Fouad

Benha University

Article

Keywords: Corrosion inhibition, carbon steel A283C, Potato peel, Adsorption, Impedance

Posted Date: June 27th, 2026

DOI: https://doi.org/10.21203/rs.3.rs-9807246/v1

License: This work is licensed under a Creative Commons Attribution 4.0 International License.
Read Full License

Additional Declarations: No competing interests reported.

Version of Record: A version of this preprint was published at Scientific Reports on October 9th, 2026. See the published version at https://doi.org/10.1038/s41598-026-68415-8.

Potato Peel Extract as an ecologically conscious Inhibitor for corrosion of A283 Carbon Steel in Hydrochloric Acid: Experimental and Theoretical Perspectives

Metwally Abdallah[1], Dina Walid[1], Omar A. Hazazi[1], Salih S. Al-Juaid[2] , Doaa F. Seyam[1] ,Ali Y. El-Etre[1], Elsayed M. Mabrouk[1], Nahed Fouad[1]

[1]Chemistry Department, Faculty of Science, Benha University, Benha, Egypt.
[2]Chemistry Department, Faculty of Applied Sciences, Umm Al-Qura University, Makkah, Saudi Arabia.
[3]Chemistry Department, Faculty of Science, King Abdulaziz University, Jeddah, Saudi Arabia.

* Corresponding authors
Prof. Dr. Metwally Abdallah: metwalli.abdelsaid@ fsc.bu.edu.eg
metwally555@yahoo.com

Abstract

Potato peel extract was validated as a safe and eco-friendly corrosion inhibitor for the carbon steel A283 grade C (CS A283) in 2.0 M HCl solution employing both chemical and electrochemical methods. The active constituents were successfully extracted using an alcoholic medium, and their chemical structures were identified by FT-IR, ^{1}H NMR, ^{13}C NMR, and mass spectrometry analyses. The findings demonstrated that the corrosion rate dramatically dropped and the inhibition efficiency rose in tandem with an increase in potato peel extract content and decline in temperature. Polarization data suggested that the potato peel extract functioned as a mixed-type inhibitor. The inhibition mechanism is attributed to the spontaneous and parallel adsorption of the extract's main constituents onto the surface of CS A283 leading to the formation of an effective protective film against the corrosive acidic medium. The adsorption process is subjected to Langmuir isotherm. Furthermore, activation and adsorption thermodynamic parameters were evaluated and discussed. Several thermodynamic activation functions were determined and analyzed to better understand the corrosion and inhibition behavior. Scanning electron microscopy (SEM) was emploed to analyze the surface morphological characteristics, affording a thorough understanding of the state of the surface and the degree of corrosion protection. The theoretical results indicated that the active constituents of potato peel extract can absorb onto the CS A283 surface. In addition, the study anticipates that petunidin and chlorogenic acid exhibit greater inhibition efficacy compared to the other components.

Keywords: Corrosion inhibition, carbon steel A283C, Potato peel, Adsorption, Impedance.

1. Introduction

Carbon steel is utilized extensively in a variety of industries of strategic and economic importance, such as oil and gas pipelines, construction, the formation of storage tanks, silos, forgings, decorative engineering, agricultural equipment and many other industrial applications. [1,2]. Hydrochloric acid (HCl) is commonly applied in pickling processes to eliminate rust from steel surfaces and enhance corrosion protection. However, during pickling, steel is exposed to highly aggressive chloride ions that can infiltrate pores and micro-cracks in the oxide film, eventually causing substrate corrosion. Several approaches have been developed to mitigate corrosion of steel in HCl media [3,4]. Among them, the use of corrosion inhibitors is thought to be one of the most effective and popular techniques.[5].

Most of corrosion inhibitors are organic compounds that include heteroatoms [6-15]. These compounds resist corrosion by adhering to the steel surface via heteroatoms, conjugated double bonds, or aromatic rings in their molecular structures. Additionally, the adsorption of these

heteroatom-including compounds on the steel surface is impacted by the chemical structure of the inhibitor, the nature and charge of the metal surface, and the kind of corrosive solution. Although organic inhibitors are characterized by their high inhibition efficiency, but most of them are toxic and environmentally harmful. This limitation has encouraged researchers to explore eco-friendly alternatives such as plant extracts and natural oils to reduce corrosion[16-21] .These green inhibitors are advantageous due to their biodegradability, low toxicity, safety for human use, and relatively low cost, which enhances their economic feasibility. In addition, they are rich in active functional groups that facilitate strong adsorption onto metal surfaces, leading to improved corrosion inhibition efficiency.

Prior studies have demonstrated that natural aqueous plant extracts and essential oils like cinnamon extract [22], Lawsonia extract [23], curcumin, parsley, and cassia bark extracts [24], as well as natural oils like mentha oil [25], lettuce oil [26], and nutmeg oil [27], significantly inhibit steel corrosion in acidic media. The fundamental way that these natural inhibitors work is by adhering to the steel surface and creating a barrier of defense. The existence of active functional groups in their chemical structures, which enable robust interactions with the steel surface, has a substantial impact on the effectiveness of inhibition.

To achieve the strategic goal of this study, the primary chemicals in potato peels were extracted using alcohol and examined as a safe, affordable, and environmentally friendly sustainable corrosion inhibitor for carbon steel A283 grade C in a 2.0 M HCl solution at varying temperatures. The inhibitory efficacy of the extract was determined by weight loss (WL), potentiodynamic polarization (PDP), and electrochemical impedance spectroscopy (EIS). A activation and adsorption parameters were also computed and analysed. The structural features and protective characteristics of the potato peel extract were examined using DFT simulations. This detailed method seeks to clarify the intricate relationships between the components of potato peels extract and the steel surface, providing insightful information to aid in the creation of effective and high-performing corrosion control techniques.

2. Experimental procedures

The carbon steel A283 grade C (CS A283) plate utilized in the current study has the following chemical composition (wt.%): 0.280 C, 0.200 Cu, 0.038 P, 1.01 Mn, 0.277 Si, 0.047 S, with the balance being Fe.”Before to each experiment, the steel specimens are manually polished using

silicon carbide (SiC) abrasive sandpaper of different grit sizes (400–1200) . The specimens are then thoroughly rinsed with distilled water and degreased with acetone before being permitted to air dry at room temperature.The chemicals used in this study were hydrochloric acid (34%), ethanol (99%), and acetone, all of which were purchased from Al-Nasr Chemicals Co., Egypt.

The potato peels were thoroughly washed, sun-dried, and then refluxed for three hours using ethanol (99%). After refluxing, the mixture was filtered, and the filtrate was concentrated. The resulting concentrate was further dried in open air to obtain the final extract as a white powder. The chemical composition of the extract was characterized using FT-IR, ^{1}H NMR, ^{13}C NMR, and mass spectrometry (MS) to identify the main active components [28].Depending on the relative proportions of its constituents, the major bioactive compounds present in potato peel include α-chaconine, chlorogenic acid, caffeic acid, petunidin, gallic acid, and quercetin (Table 1). In addition, potato peel contains moisture, proteins, ash, and starch, along with smaller amounts of α-solanine and demissidine. It also includes several phenolic and flavonoid compounds such as pelargonidin, peonidin, malvidin, p-coumaric acid, ferulic acid, protocatechuic acid, rutin, and catechin. Moreover, it is a source of fatty acids, essential minerals (including zinc, potassium, sodium, calcium, iron, and magnesium), as well as vitamins such as B-complex vitamins and vitamin C (ascorbic acid) [29–31]. An amount of 1000 mg of the extract was dissolved in 1 L of distilled water to obtain the stock solution, from which the desired concentrations were prepared by serial dilution.

Table (1): The primary active ingredients in potato peel extract

Name	Content (µg/g)	Chemical Structure	Formula and M.W (g/mol)
α-chaconine	670 ± 130	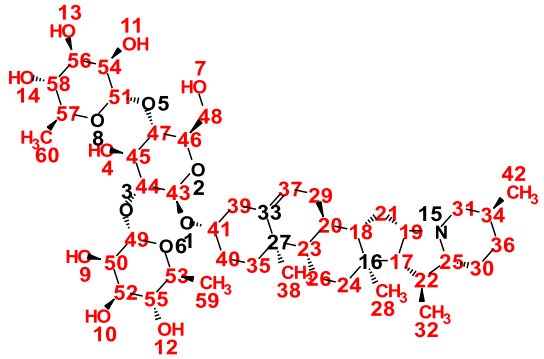	$C_{45}H_{73}NO_{14}$ 852.07

Name	Content (µg/g)	Chemical Structure	Formula and M.W (g/mol)
Chlorogenic acid	9.05 ± 0.015	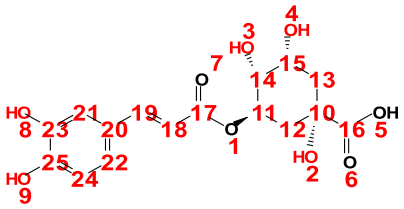	$C_{16}H_{18}O_9$ 354.31
Caffeic acid	6.97 ± 0.001	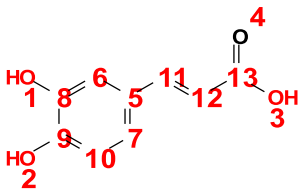	$C_9H_8O_4$ 180.16
Petunidin	3.23 ± 0.022	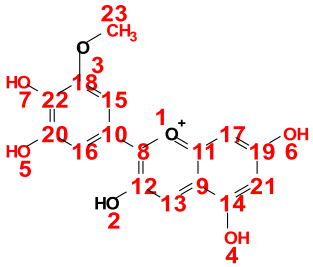	$C_{16}H_{13}ClO_7$ 352.72
Gallic acid	1.91 ± 0.002	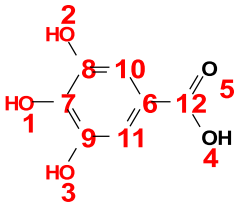	$C_7H_6O_5$ 170.12
Quercetin	0.42 ± 0.03	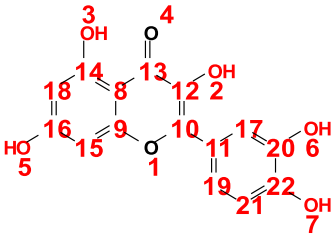	$C_{15}H_{10}O_7$ 302.24

2.2. Clarification of inhibitors

FT-IR in **Figure (1-a)** is acquired by Thermos Nicolet IS10 FT-IR Spectrophotometer. IR spectrum (KBr) showed characteristic bands at 3413-3212 cm^{-1} (ν_{OH}), 3036 cm^{-1} (ν_{CH} Ar), 2949 cm^{-1} (ν_{CH} Alkane), 1697 cm^{-1} ($\nu_{C=O}$), 1636 cm^{-1} ($\nu_{C=C}$ Ar), 1513 cm^{-1} (ν_{C-H}), 1290-1202 cm^{-1} (ν_{C-O}), 1170-1085 cm^{-1} (ν_{C-N}), 1018 cm^{-1} (ν_{C-O-C}).

^{1}H NMR and **^{13}C NMR** both are acquired by Mercury, temperature of 30°C, 300 MHz for ^{1}H NMR and 75.46 MHz for ^{13}C NMR, CD_3OD as a solvent.

^{1}H NMR (300 MHz, CD_3OD) δ:

α-chaconine: 4.97 – 4.90 (m, 3H, 12, 14, 37), 4.58 – 4.49 (m, 4H, 10, 11, 13, 43, 49, 51), 4.05 – 3.97 (m, 3H, 9), 3.92 – 3.73 (m, 7H, 41, 44, 45, 46, 47, 48'', 50, 52, 56), 3.64 – 3.53 (m, 3H, 48', 53, 54, 57), 3.57 – 3.49 (m, 3H, 4), 3.38 – 3.28 (m, 2H, 19, 55, 58), 2.96 – 2.84 (m, 2H, 25, 31), 1.99 – 1.83 (m, 3H, 21'', 29'', 30'', 39, 40''), 1.82 – 1.24 (m, 19H, 7, 17, 18, 20, 21', 22, 23, 24, 26, 29', 30', 34, 35, 36, 40'), 1.11 – 1.06 (m, 5H, 59, 60), 1.00 – 0.97 (s, 2H, 38), 0.97 – 0.87 (m, 7H, 32, 42), 0.80 – 0.77 (s, 2H, 28).

Chlorogenic acid: 7.58 – 7.51 (m, 1H, 19), 7.34 – 7.28 (d, *J* = 16.3 Hz, 1H, 18), 7.10 – 7.06 (s, 1H), 7.05 – 7.01 (d, *J* = 2.1 Hz, 1H, 21), 6.97 – 6.92 (dd, *J* = 8.5, 2.1 Hz, 1H, 22), 6.80 – 6.75 (d, *J* = 8.4 Hz, 1H, 24), 5.75 – 5.72 (s, 1H, 2), 5.43 – 5.35 (ddt, *J* = 8.0, 7.0, 4.0 Hz, 1H, 11), 5.15 – 5.11 (s, 1H, 9), 4.70 – 4.65 (d, *J* = 6.0 Hz, 1H, 4, 8), 4.12 – 4.03 (dddt, *J* = 9.9, 6.2, 5.1, 2.5 Hz, 1H, 15), 3.76 – 3.68 (ddd, *J* = 8.2, 6.0, 4.9 Hz, 1H, 14), 3.60 – 3.55 (d, *J* = 5.9 Hz, 1H, 3), 2.50 – 2.43 (m, 1H, 12'), 2.29 – 2.18 (m, 2H, 12'', 13''), 2.04 – 1.97 (dd, *J* = 14.2, 5.0 Hz, 1H, 13').

Caffeic acid: 7.45 – 7.38 (m, 1H, 11), 7.10 – 7.06 (s, 1H, 1), 7.05 – 7.01 (d, *J* = 2.1 Hz, 1H, 6), 6.97 – 6.92 (dd, *J* = 8.5, 2.1 Hz, 1H, 7), 6.80 – 6.75 (d, *J* = 8.4 Hz, 1H, 10), 6.33 – 6.26 (d, *J* = 16.5 Hz, 1H, 12), 5.15 – 5.11 (s, 1H, 2, 3).

Petunidin: 9.80 – 9.79 (s, 1H, 4), 9.42 – 9.40 (s, 1H, 6), 8.21 – 8.20 (s, 1H, 13), 7.93 – 7.92 (s, 1H, 7), 7.79 – 7.76 (m, 3H, 5, 16), 7.70 – 7.69 (d, *J* = 1.4 Hz, 1H, 15), 6.83 – 6.81 (d, *J* = 2.3 Hz, 1H, 21), 6.72 – 6.70 (d, *J* = 2.4 Hz, 1H, 17), 3.83 – 3.82 (s, 3H, 23).

Gallic acid: 8.31 – 8.30 (s, 2H, 1, 2, 3), 6.93 – 6.93 (s, 2H, 10, 11), 6.87 – 6.86 (s, 1H).

Quercetin: 8.39 – 8.37 (s, 1H, 6, 7), 7.64 – 7.62 (d, *J* = 2.1 Hz, 1H, 17), 7.55 – 7.50 (dd, *J* = 8.7, 2.1 Hz, 2H, 19), 6.84 – 6.80 (d, *J* = 8.7 Hz, 1H, 21), 6.73 – 6.71 (s, 1H, 5), 6.35 – 6.32 (d, *J* = 1.8 Hz, 2H, 3, 15), 6.21 – 6.19 (d, *J* = 2.0 Hz, 2H, 2, 18).

^{13}C NMR (75.46 MHz, CD_3OD) δ:

α-chaconine: 141.00, 33, 121.92, 37, 102.72, 51, 101.99, 49, 100.46, 43, 78.70, 47, 78.46, 44, 78.35, 41, 77.45, 45, 77.24, 46, 74.74, 25, 73.91, 58, 73.82, 55, 72.54, 54, 72.43, 56, 72.34, 52, 72.24, 50, 70.01, 57, 69.91, 53, 69.13, 19, 62.95, 17, 61.77, 48, 60.27, 31, 57.63, 18, 40.41, 16, 40.09, 24, 39.05, 39, 37.61, 35, 37.56, 27, 36.86, 22, 33.40, 21, 32.40, 29, 31.99, 20, 31.85, 36, 31.34, 34, 30.24, 40, 29.29, 30, 21.16, 26, 19.82, 42, 19.29, 38, 18.51, 60, 18.42, 59, 18.34, 32, 16.82, 28.

Chlorogenic acid: 177.63, 16, 167.45, 17, 148.44, 25, 147.18, 23, 146.72, 19, 127.43, 20, 122.94, 22, 116.50, 24, 116.04, 18, 115.30, 21, 75.95, 10, 72.78, 14, 72.59, 11, 71.49, 15, 38.80, 12, 38.21, 13.

Caffeic acid: 169.48, 13, 148.44, 9, 147.03, 8, 145.86, 11, 126.53, 5, 122.67, 7, 117.44, 12, 116.17, 10, 114.84, 6.

Petunidin: 169.77, 19, 161.31, 8, 158.06, 14, 156.03, 11, 151.45, 18, 148.73, 20, 145.11, 22, 143.48, 12, 132.27, 13, 122.51, 10, 113.47, 9, 112.59, 16, 108.63, 15, 103.22, 21, 95.22, 17, 56.70, 23.

Gallic acid: 169.44, 12, 145.77, 8, 9, 139.16, 7, 121.70, 6, 109.87, 10, 11.

Quercetin: 177.73, 13, 165.19, 16, 160.90, 14, 157.73, 9, 148.61, 22, 147.39, 10, 145.57, 20, 136.39, 12, 122.61, 11, 120.87, 19, 115.95, 21, 115.73, 17, 103.29, 8, 99.64, 18, 94.45, 15.

Molecule fragments for **mass Spectrum** were acquired by Thermo Scientific, USA, Trace GC Ultra/ISQ Single Quadrupole MS, TG-5MS detection. The molecules' mass ranged from 50 to 900 a.m.u., and their ionization voltage was 70 eV.

Mass Spectrum (EI-MA): m/z ($C_{45}H_{73}NO_{14}$) calcd = 852.09 (0.73%) [M^+], m/z ($C_{16}H_{18}O_9$) calcd = 354.83 (2.37%) [M^+], m/z ($C_9H_8O_4$) calcd = 180.01 (29.18%) [M^+], m/z ($C_{16}H_{13}O_7$) calcd = 317.16 (3.08%) [M^+], m/z ($C_7H_6O_5$) calcd = 170.91 (7.07%) [M^+], and m/z ($C_{15}H_{10}O_7$) calcd = 302.03 (2.36%) [M^+] are shown in **Figure (1-b)**.

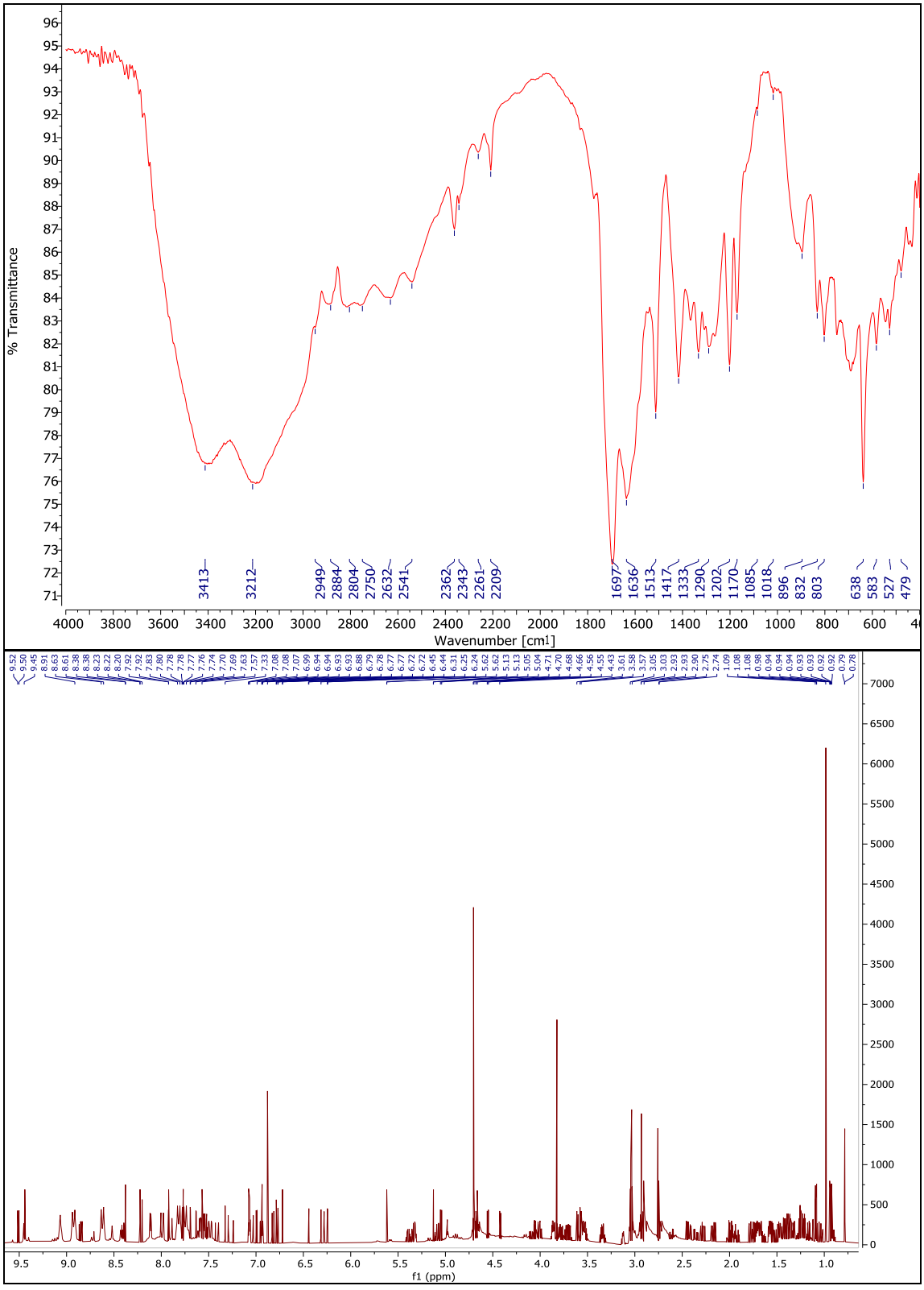

Figure (1-a): FT-IR and ^{1}H NMR of the extracted main active potato peel compounds

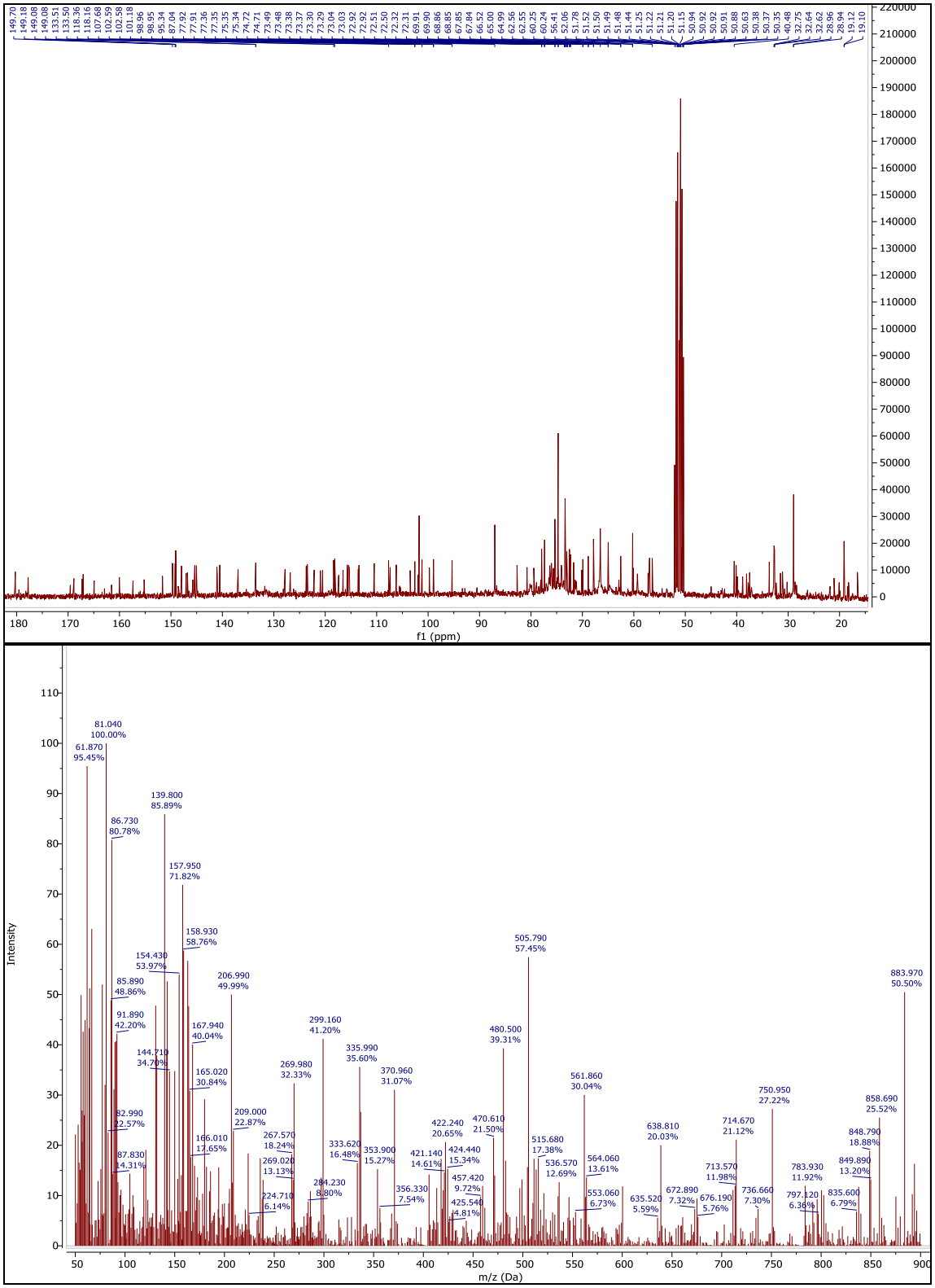

Figure (1-b): ^{13}C NMR and mass spectra of the extracted main active potato peel compounds

2.3.Corrosion measurements

The weight loss (WL)measurements were done using CS A283 coupons of 1 × 1 × 1 cm^3 dimensions in 2.0 M HCl solution without and with 10, 50, 100, 150, 300, 400 and 500 ppm of potato peel extract, at 25°C±1. These measurements were recorded daily over a period of 7 days. The WL experiments were conducted according to the previously outlined procedures [31].

Utilizing an SP-150 Potentiostat with EC-Lab software, potentiodynamic polarization (PDP) curves and electrochemical impedance spectroscopy (EIS) of CS A283in 2.0 M HCl solution with and without the relevant concentrations of potato peel extract were identified. These electrochemical tests were repeated with and without 500 parts per million potato peel extract at various temperatures ranging from 25 to 50ºC

Prior to every experiment, the electrode is submerged in the corrosive HCl media for 15 minutes to guarantee the stability of the electrode potential. After then, the run is performed in relation to the open circuit potential. The scan rate used in PDP was 1.0 mV/s and the frequency range for EIS was from 100 kHz to 0.1 Hz, with 10 mV signal amplitude
The double layer capacitance is determined according to the coming equation [32]:

$$C_{dl} = Y_O w^{N-1} = Y_O (2\pi f_{max})^{N-1} \quad (1)$$

where, R_{ct} and $R_{ct,ext}$ are the charge transfer resistance of corrosion reaction without and with potato peel extract. Y_0 is the constant phase element in $S.s^N$, f_{max} is the frequency at which the imaginary component of the impedance is maximal.

2.4.Evaluation of corrosion inhibition efficiency

. The inhibition efficiency (η) and surface coverage (θ) of the investigated potato peel extract were determined from WL and PDP measurements using the following equations [33]:

$$\eta = \left(1 - \frac{\alpha}{\beta}\right) \times 100 \quad (2)$$

$$\eta = \left(1 - \frac{\alpha}{\beta}\right) \quad (3)$$

In this context, α and β refer to the corrosion rate and corrosion current density derived from WL and PDP measurements, respectively, for CS A283in 2.0 M HCl solution with and without potato peel extract.. In contrast, for EIS analysis, α and β correspond to the charge transfer resistance (R_{ct}) values of the blank solution and the inhibited solution, respectively.

2.5.Surface analysis

A JSM-IT700HR/LA scanning electron microscope (SEM) was employed to analyze the surface morphologies of CS A283. For specimens that had just been surface polished, the micrographs were taken at an accelerating voltage of 15 kV following a 6-hour immersion in a 2.0 M HCl solution.both in the devoid of and including of 500 ppm of the extract. All images were recorded at a magnification of 1500×

2.6. Quantum and Monte Carlo simulations

Gaussian 09 was applied for determining quantum parameters. The optimal geometric structure of the potato peel's active molecules was discovered using the DFT: B3LYP/6-311G(d,p) technique. Materials Studio 2020's Universal Force-Field was used to conduct a Monte Carlo simulation. It was accomplished in a (31.55 × 31.33 × 16.31 Å) simulation boundary box with a (5 × 5) supercell and a 35Å slab thickness.20 molecules of H_2O and HCl were inserted in the simulation box to simulate the solvent on Fe (110) surface.

3. Results and Discussion

3.1. Weight loss (WL) measurements

Figure 2 depicts the time-dependent behavior of the corrosion rate (CR) and inhibition efficiency (η), whereas the corresponding computed values of CR and η are compiled in Table (2).

The findings reveal that the corrosion rate of CS A283 increases over time owing to the slow disintegration of the created iron oxide layer. A red, porous layer develops on the surface while rusting, on the surface, and it finally becomes loose and powdery. Although the performance of potato peel extract on CS A283 decreases with prolonged exposure,, it still retains an efficiency of 20.5% at a concentration of 500 ppm after 7 days.

The inhibitory influence of potato peel extract diminishes with increasing immersion time due to the adsorbed protective layer on the steel surface progressively becomes less stable. While aggressive hydrogen and chloride ions penetrate the protective barrier and target the CS A283 surface, some inhibitor molecules desorb from the steel surface after prolonged contact with the acidic medium. Additionally, the adsorbed organic molecules may eventually dissolve or disintegrate, reducing the surface coverage and, hence, decreasing the inhibitory efficiency.

The addition of potato peel extract considerably lowers the corrosion rate of CS A283

in 2.0 M HCl solution, with the inhibition effect becoming more pronounced as the extract concentration increases. This effect is caused by the increased availability of active molecules at higher concentrations, which enhances their adsorption onto the steel surface and produces a more resistant and denser. The finding that the inhibition efficacy rises with increasing extract amount thus confirms the potato peel extract's efficacy as a corrosion inhibitor in acidic medium [34].

The molecular structures of the potato peel extract's active ingredients, which are rich in heteroatoms like N and O as well as conjugated π-electron systems and aromatic rings, are largely responsible for the extract's inhibitory effectiveness. Through donor-acceptor interactions between the unoccupied d-orbitals of iron atoms and the lone pair electrons of heteroatoms, these structural characteristics improve the extract molecules' capacity to adsorb firmly onto the steel surface. Furthermore, the adsorption process is further stabilized by π–d orbital interactions. This reduces the number of active corrosion sites and greatly inhibits both anodic metal dissolution and cathodic hydrogen evolution reactions by forming a protective adsorbed film that successfully isolates the steel surface from the aggressive HCl medium [35].

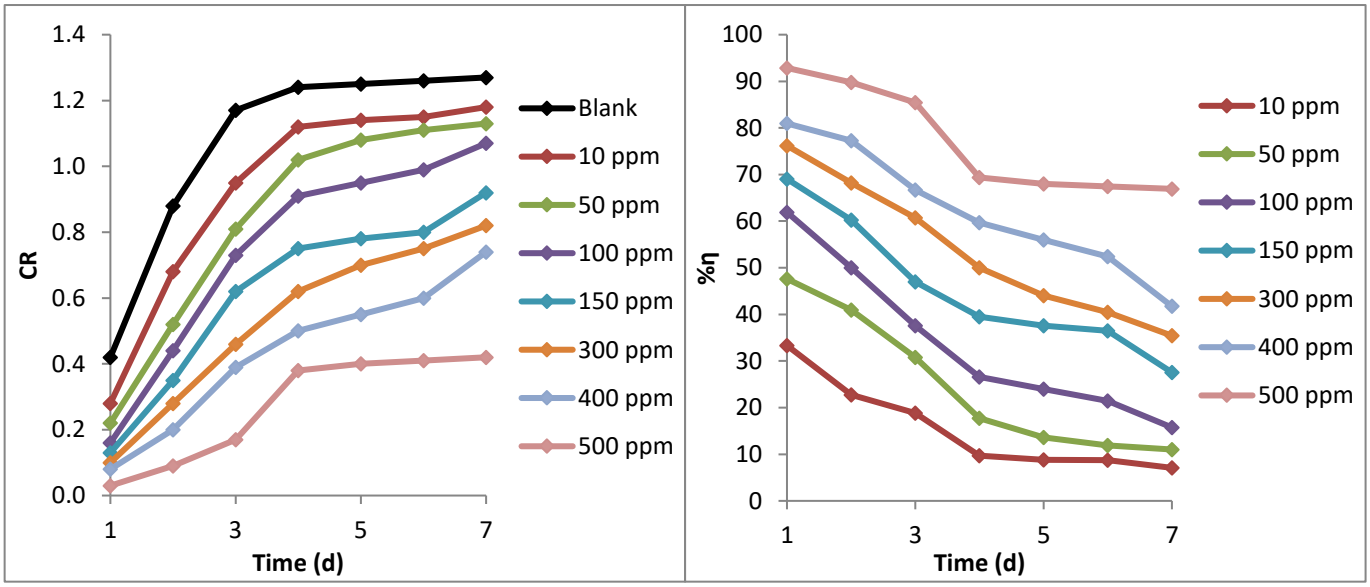

Figure (2): Effect of exposure time on the corrosion rate of CS A283 and inhibition efficiency of potato peel extract in 2.0 M HCl solution

Table (2): Variation of corrosion rate (CR, $g \cdot d^{-1} \cdot cm^{-2}$) for CS A283 in 2.0 M HCl solution with and without extract at various concentrations and exposure durations at 298 K.

Solution	1 (d)		2 (d)		3 (d)		4 (d)		5 (d)		6 (d)		7 (d)	
(ppm)	CR	η	CR	η	CR	η	CR	η	CR	η	CR	η	CR	η
Blank	0.42	-	0.88	-	1.17	-	1.24	-	1.25	-	1.26	-	1.27	-
10	0.28	33.3	0.68	22.7	0.95	18.8	1.12	9.7	1.14	8.8	1.15	8.7	1.18	7.1
50	0.22	47.6	0.52	40.9	0.81	30.8	1.02	17.7	1.08	13.6	1.11	11.9	1.13	11.0
100	0.16	61.9	0.44	50.0	0.73	37.6	0.91	26.6	0.95	24.0	0.99	21.4	1.07	15.7
150	0.13	69.0	0.35	60.2	0.62	50.5	0.75	39.5	0.78	37.6	0.80	36.5	0.92	27.6
300	0.10	76.2	0.28	68.2	0.46	60.7	0.62	50.0	0.70	44.0	0.75	40.5	0.82	35.4
400	0.08	80.9	0.20	77.3	0.39	66.7	0.50	59.7	0.55	56.0	0.60	52.4	0.74	41.7
500	0.03	92.8	0.09	89.8	0.17	85.5	0.38	69.4	0.42	66.4	0.48	61.9	0.42	66.9

3.2. Potentiodynamic polarization (PDP) measurements

PDP curves of CSA283 in blank 2.0 M HCl solution and in the presence of varying concentrations of potato peel extract were recorded at a scan rate of 1.0 mV s^{-1}.The resulting polarization curves are displayed in Figure (3). The corrosion kinetic parameters, including corrosion potential (E_{corr}), corrosion current density (i_{corr}), anodic Tafel slope (β_a) and cathodic Tafel slope (β_c) deduced from these curves and are summarized in Table (3).

The findings unequivocally demonstrate that raising the concentration of potato peel extract led to both a significant improvement in inhibitory effectiveness and a substantial decline in the rate of corrosion. The progressive increase in the number of inhibitor molecules in the solution, which promotes greater adsorption onto the CS A283 surface. As the surface coverage increases, a more compact and shielding absorbed coating is created, effectively blocking the active corrosion sites and limiting the engagement between the CS A283 and the aggressive acidic environment. The increasing quantity of inhibitor molecules in the solution, which encourages increased absorption on the surface of CS A283 leading to increased surface coverage and the formation of a denser and more effective absorbent layer, which inhibits active corrosion sites and reduces metal friction with corrosive acidic environments.

Furthermore, analysis of the PDP curves reveals that each anodic and cathodic branch moves in the direction of lower current density values upon the addition of the extract. This behavior indicates that the potato peel extract operates as a mixed-type inhibitor, effectively reducing both

the anodic steel dissolution and the cathodic hydrogen evolution reactions. The values of βc and βa for the extract under investigation demonstrate comparatively slight shifts toward more negative and more positive potentials. The Tafel slopes (βc and βa) had changed by approximately 5 mV dec^{-1} and 3 mV dec^{-1}, respectively, when compared to the blank solution. These minor variations imply that the potato peel extract mostly operates as a mixed-type inhibitor, preventing both anodic and cathodic processes without significantly altering the corrosion mechanism. Furthermore, the values E_{corr}. remains nearly unchanged, showing a small displacement of about 34 mV compared to the blank solution. This limited shift further supports the conclusion that the potato peel extract acting as a mixed-type corrosion inhibitor [36].

The declining I_{corr} values and rising inhibition efficacy (IE%), reflect the potent inhibitive performance of the potato peel extract. This behavior can be attributed to the adsorption of the extract molecules onto the surface of CS A283, where they form a protective layer by occupying active sites. The presence of functional groups within the extract facilitates this adsorption process, thereby reducing the corrosion rate and enhancing the overall inhibition efficiency

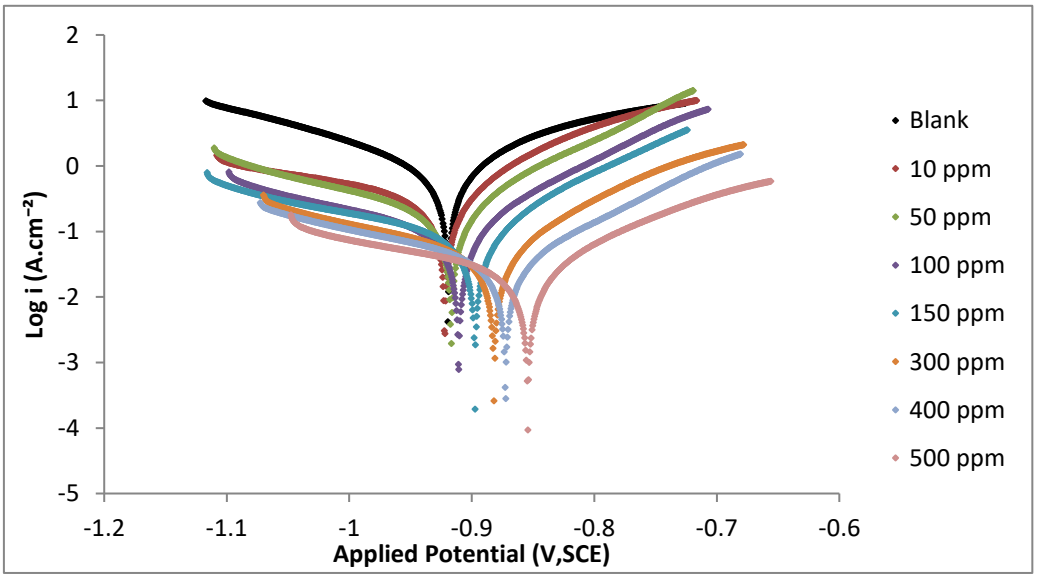

Figure (3): PDP curves of CS A283 without and with different extract concentrations in 2.0 M HCl solution, and at 298 K

Table (3): PDP parameters of CS A283 without and with different extract concentrations in 2.0 M HCl solution, and at 298 K

Solution (ppm)	β_c (mV/dec)	β_a (mV/dec)	E_{corr} (mV)	i_{corr} (mA /cm^2)	CR (mm/y)	R_P (Ω)	η_{PDP}
Blank	-131	95	-919	751.13	99.27	0.32	-
10	-133	96	-921	229.68	30.36	1.0	69.42
50	-133	96	-916	161.12	21.29	1.5	78.55
100	-134	97	-910	78.53	10.38	3.0	89.55
150	-135	97	-907	67.66	8.94	3.5	90.99
300	-135	98	-898	37.56	4.96	6.4	95.00
400	-136	98	-890	29.05	3.84	8.3	96.13
500	-136	98	-885	15.95	2.11	15.1	97.88

3.3.Electrochemical impedance spectroscopy (EIS) measurements

The EIS behavior of CS A283 in 2.0 M HCl is illustrated in Figure (4) using Nyquist and Bode diagrams, recorded both without the inhibitor and after the addition of certain concentrations of potato peel extract. Table (4) summarizes the corresponding EIS parameters, such as the solution resistance (R_s), the capacity of double layer (C_{dl}), and the charge transfer resistance (R_{ct}), which represents the resistance to electron transfer at the steel/solution contact. The impedance data was also employed to determine the inhibitory efficacy (η) values. The lower chi-square (χ^2) values, on the order of 10^{-4}, reflect excellent alignment between the experimental data and the fitted model. The impedance parameters were derived by fitting the experimental spectra to the Randles equivalent electrical circuit, as seen in Figure (4).This circuit consists of the solution resistance (R_s) connected in series with a parallel combination of the double-layer capacitance (C_{dl}) and the charge transfer resistance (R_{ct}).

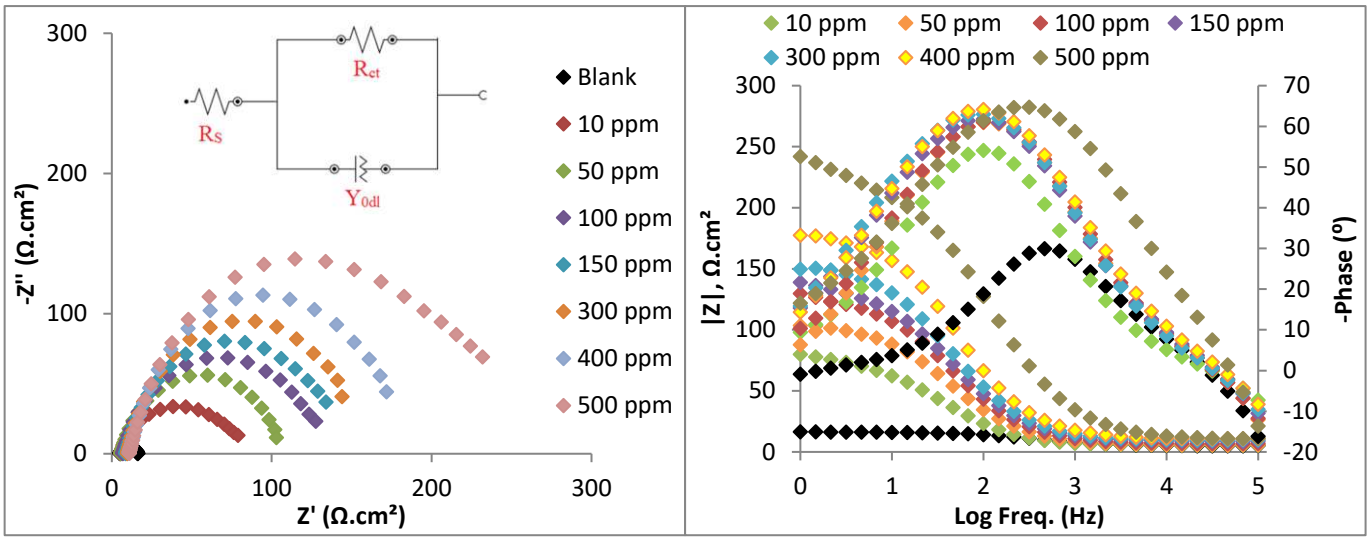

Figure (4): (a) Nyquist and (b) Bode diagrams (c) The equivalent circuit for CS A283 in blank 2.0 M HCl solution and with varying concentrations of potato peel extract, at 298 K.

The Nyquist impedance charts display depressed (non-ideal) semicircles rather than perfect ones. This behavior is often associated with frequency dispersion of the interfacial impedance, which is induced by surface heterogeneity, roughness, grain boundaries, adsorption of inhibitor molecules, formation of porous surface layers, and the existence of impurities or non-uniform electrode surfaces [37].

The existence of semicircular profiles in the presence and absence of various extract concentrati on implies that a charge transfer mechanism is primarily responsible for the corrosion process of CS A283 in 2.0 M HCl [38].Additionally, increased corrosion resistance is indicated by the obse rved rise in the capacitive loop's width with increasing extract concentration, and gradual strengthening of a protective inhibitive layer on the steel surface. The diameter of the high-frequency semicircle, which stands for the charge transfer resistance (R_{ct}), and the double-layer capacitance (C_{dl}) are the two main characteristics that were taken from the Nyquist plots.A careful examination Table (4) reveals that raising the potato peel extract concentration causes a noticeable rise in charge transfer resistance (R_{ct}), accompanied by an improvement in inhibitory efficiency (%η). This behavior is attributed to the adsorption of the extract on the steel /solution interface, resulting in the creation of a stable and protective film. Concurrently, as the concentration of extract increases, the C_{dl} values fall. This drop may be explained by the adsorbed extract gradually displacing water molecules, changing the interfacial structure and lowering the local dielectric constant at the steel/solution contact [39] . Consequently, the formation of this adsorbed layer improves surface coverage and corrosion protection

The Bode plots show that adding potato peel extract mainly affects the intermediate and low-frequency regions. While the high-frequency response (linked to solution resistance, Rs) remains nearly unchanged, the impedance modulus (|Z|) increases with higher extract concentration. This increase reflects a rise in R_{ct}, indicating that corrosion is suppressed as a protective adsorbed layer forms and hinders electron transfer at the steel/solution interface. Additionally, the widening of the phase-angle peak over a wider frequency range implies that the inhibitor film covers a larger portion of the surface and improves surface uniformity. This improved surface homogeneity reduces heterogeneity, limits the formation of localized corrosion sites, and strengthens the barrier properties of the protective layer. Furthermore, when the concentration of potato peel extract rises, the phase-angle peaks move to higher values and go closer to the ideal capacitor values (−90°), suggesting a more compact and orderly adsorption of extract molecules on the steel surface [40].

Overall, the Bode diagram confirms that higher concentrations of potato peel extract enhances stronger adsorption, leading to the building of a more stable and protective film. This results in enhanced corrosion inhibition efficiency by increasing the resistive and capacitive characteristics of the steel/solution interface.

Table (4): EIS parameters of A283 carbon steel in blank 2.0 M HCl solution and in the existence of various concentrations of potato peel extract at 298 K.

Solution (ppm)	n	Y_{0dl} (µS.s^N)	C_{dl} (µF)	R_S (Ω)	R_{ct} (Ω)	η
Blank	0.87	9.9	114.1	4.91	11.52	-
10	0.80	7.5	90.4	5.40	73.51	84.32
50	0.85	6.0	81.3	5.61	97.27	88.15
100	0.85	5.5	79.7	6.76	120.79	90.46
150	0.86	4.9	66.4	8.67	125.35	90.81
300	0.88	3.6	58.4	9.79	134.23	91.41
400	0.86	2.4	47.2	10.77	161.05	92.84
500	0.90	1.5	32.7	11.00	220.91	94.78

3.4. Assessment of corrosion kinetics under varying temperatures

Temperature plays a crucial role in controlling both the corrosion rate and the adsorption characteristics of potato peel extract on the CS A283 surface. To assess its influence on inhibition performance, PDP measurements were conducted across a temperature range of 25 °C to 50 °C. Figure 5 presents the PDP curves of CS A283 in 2.0 M HCl solution at selected

temperatures, both in the devoid of and including 500 ppm potato peel extract. Tables 5 summarize the corresponding PDP parameters for CS A283 under the same conditions.

The PDP curves show comparable patterns at all examined temperatures, both with and without potato peel extract, according to an analysis of the findings. This consistency implies that the corrosion reaction mechanism is not much varied by either raising the temperature or adding the extract. This finding is further supported by the of $E_{corr.}$, βa and βc values remain nearly constant under all investigated conditions [41].

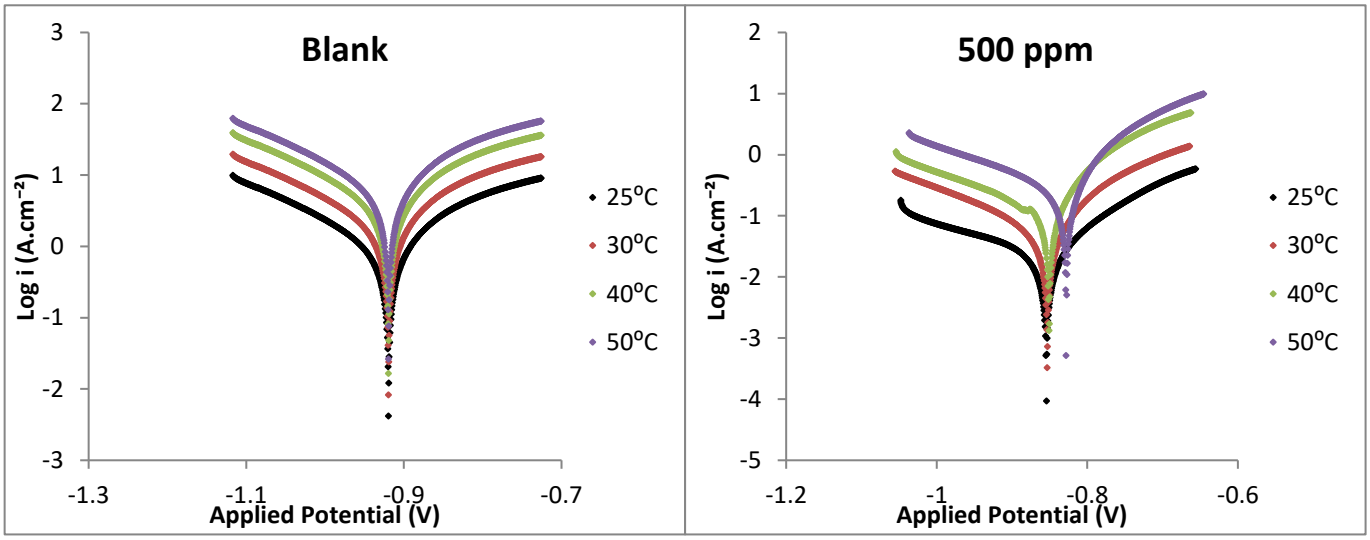

Figure 5: PDP curves of corrosion of CS A283 in blank and inhibited 2.0 M HCl with 500 ppm potato peel extract

Analyzing this figure5 and table 5 reveal that the PDP curves, both with and without specific potato peel extract concentrations, show almost the same tendency at all examined temperatures. It implies that the corrosion reaction mechanism is unaffected by the temperature rise or the addition of the extract. The minimal variation in the Tafel slopes (βa and βc) and the nearly constant E_{corr} further support this tendency [42].

In both uninhibited and inhibited solutions containing 500 ppm of the extract, it was noticed that the inhibition efficiency (η) values of potato peel extract diminished with rising temperature. This reduction implies that physical adsorption is the primary mechanism by which molecules of potato peel extract adhere to the metal surface. Lower protection efficiency results from the adsorbed inhibitor molecules becoming less stable and progressively desorbing from the surface as the temperature rises. Physisorption processes frequently exhibit this tendency [43].

Table 5: PDP corrosion parameters of CS A283 in blank 2.0 M HCl solution and with500 ppm potato peel extract at different temperature

Solution	T (°C)	β_c (mV/dec)	β_a (mV/dec)	E_{corr} (mV)	i_{corr} (mA /cm^2)	CR (mm/year)	R_P (Ω)	η
Blank	25	-133	96	-919	751.1	99.2	0.32	-
	30	-133	96	-920	1498.7	198.0	0.16	
	40	-133	97	-921	2990.2	395.2	0.08	
	50	-134	97	-921	4739.3	626.3	0.05	
500 ppm	25	-134	97	-854	15.9	2.1	15.18	97.88
	30	-134	98	-853	45.7	6.0	5.29	96.95
	40	-135	98	-850	127.6	16.8	1.90	95.73
	50	-135	98	-828	253.4	33.5	0.96	94.65

The activation thermodynamic parameters, including the activation energy (E_a), the enthalpy of activation (ΔH*) and the entropy of activation (ΔS*) are determined by applying the following Arrhenius and transition state equations [44,45]:

$$ln\,CR = \left(\frac{-E_a}{RT}\right) + ln\,A \qquad (4)$$

$$ln\left(\frac{CR}{T}\right) = \left(ln\left(\frac{R}{N_A\,h}\right) + \left(\frac{\Delta S^*}{R}\right)\right) - \frac{\Delta H^*}{RT} \qquad (5)$$

Fig. 6A illustrates the plots between log CR and 1/T for the corrosion of CS A283 steel in 2.0 M HCl solution, both in the absence and presence of varying concentrations of potato peel extract. The obtained plots exhibit linear behavior, confirming Arrhenius-type dependence. From the slope of each straight line the values of (Ea*) was determined and reported in Table 6. Furthermore, the thermodynamic parameters ΔH* and ΔS* were derived from the slope and intercept, respectively, of the linear plots of log (CR/T) versus 1/T (Fig. 6B) and reported in Table 6. The R^2 values of the linear plots were around unity, signifying that the Arrhenius and transition state equation results fit the data well.These findings shed more light on the corrosion process and how the potato peel extract affects the system's thermodynamic behavior.

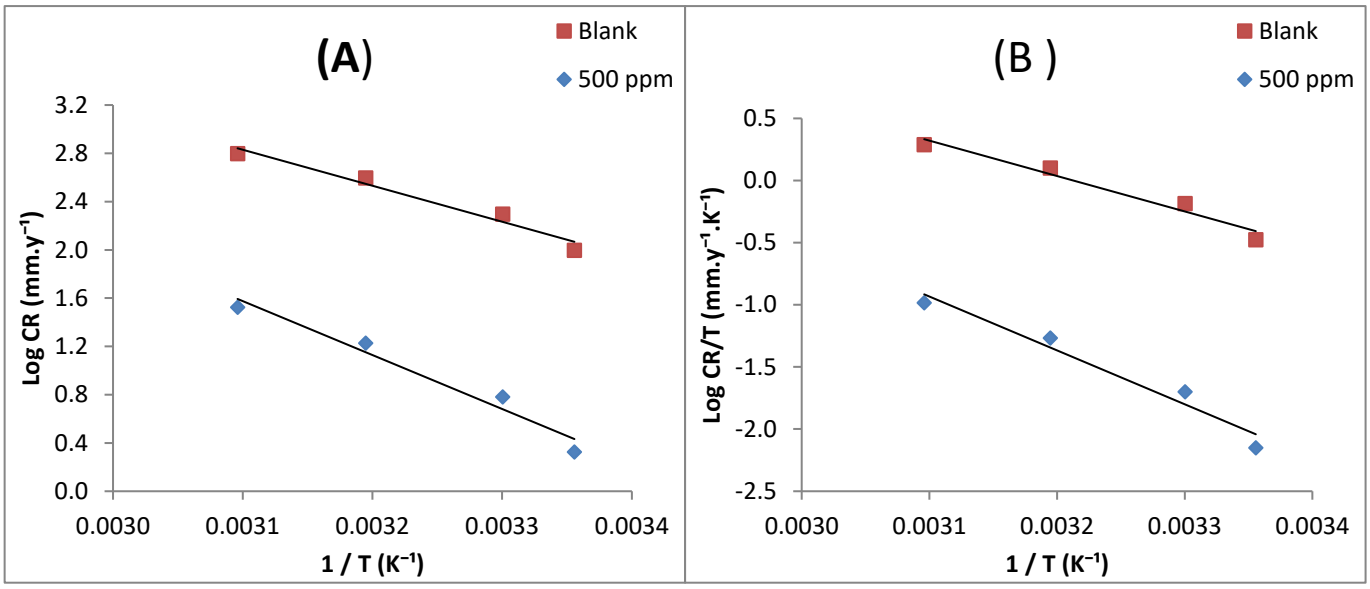

Figure 6: PDP derived (A)Arrhenius and (B) transition state plots for corrosion of CS A283 in blank 2.0 M HCl and inhibited 2.0 M HCl with 500 ppm potato peel extract

Table 6 demonstrates that the E_a values are higher when 500 ppm of potato peel extract is present. This increase in E_a indicates that the adsorbed potato peel extract molecules act as a barrier on CS A283 surface. The potato peel extract adsorbs physically onto the active sites of the CS A283 surface. These extract molecules likely contain π-electron systems and heteroatoms such as nitrogen and oxygen, which help in this adsorption process. This interaction increases the activation energy required for the corrosion reaction, making it more difficult to proceed. As a result, the system becomes more stable and shifts to a lower-energy state due to the development of a protective inhibitor layer. This layer reduces the thermodynamic favorability of corrosion and suppresses its progression.

The positive values of ΔH imply that the corrosion process of CS A283 is endothermic .This suggests that energy input is required for the dissolution of the steel to occur. The presence of potato peel extract, this process becomes less beneficial, confirming that the extract effectively hinders the corrosion of CS A283 by increasing the energy required for the reaction. The negative values of ΔS* signify that the activated complex created during the rate-determining step is more ordered than the reactants. This signifies that randomness reduces as the reaction approaches the active stage. Additionally, the extract molecules are readily adsorbed onto the steel surface, replacing the water molecules at the steel/solution contact. This way contributes to the observed entropy changes and promotes the formation of a protective adsorbed layer on the steel surface [46].

The ability of potato peel extract molecules to adhere to the steel surface at high temperatures attributed to their functional groups is demonstrated by the change in the thermodynamic parameters. The structure of potato peel molecules reveals heteroatoms such as π electrons and nitrogen and oxygen atoms, which can give electrons to the steel's empty d-orbitals and act as electrostatic attractors for the charged steel surface.

Table 6. Thermodynamic activation functions for the corrosion of A283C steel in uninhibited and inhibited 2.0 M HCl solution including 500 ppm potato peel extract, obtained from PDP measurements.

	Temp.	CR	H	E_a ($kJ.mol^{-1}$)	ΔH^* ($kJ.mol^{-1}$)	ΔS^* ($J.mol^{-1}.K^{-1}$)
Blank	298K	99.27	-	27.12	24.54	-112.35
	303K	198.07				
	313K	395.21				
	323K	626.37				
500 ppm	298K	2.11	97.88	45.58	43.00	-101.85
	303K	6.05	96.95			
	313K	16.86	95.73			
	323K	33.50	94.65			

3.5. Surface morphology,

Scanning electron microscopy **(**SEM) provides important details on surface morphology, corrosion damage, and the effectiveness of corrosion inhibitors in addition to generating high-resolution images. The resolution of SEM instruments ranges from less than 1 nanometer to several nanometers. In the present study, SEM micrographs of CS A283 immersed in 2.0 M HCl without an inhibitor show a severely degraded surface with pits, cracks, uneven corrosion products, and roughness. These features are typical of a strong acid attack, when the CS A283 dissolves rapidly, leading to localized corrosion and significant surface heterogeneity. On the other hand, the SEM images of the CS A283 surface subjected to 500 ppm potato peel extract reveal a significantly smoother and more homogeneous morphology with a noticeable reduction in pits and cracks. This improvement implies that the extract adsorbs onto the CS A283 surface

and forms a protective coating that serves as a physical barrier between the steel and the acidic medium as depicted in **Figure (7)**[47].

This adsorbed layer slows down the direct contact of H^+ ions and aggressive chloride ions (Cl^-) with the steel surface, thereby reducing the rate of steel dissolution. Furthermore, the inhibitor film likely blocks active corrosion sites and limits electron transfer reactions, which are essential for the corrosion process. The smoother appearance also suggests that the protective layer enhances surface homogeneity, lessens localized corrosion.

Overall, the SEM analyses demonstrate that potato peel extract functions as an efficient corrosion inhibitor through adsorption and film development on the CS A283 surface, significantly supporting the electrochemical findings (such as higher charge transfer resistance and decreased corrosion rate).

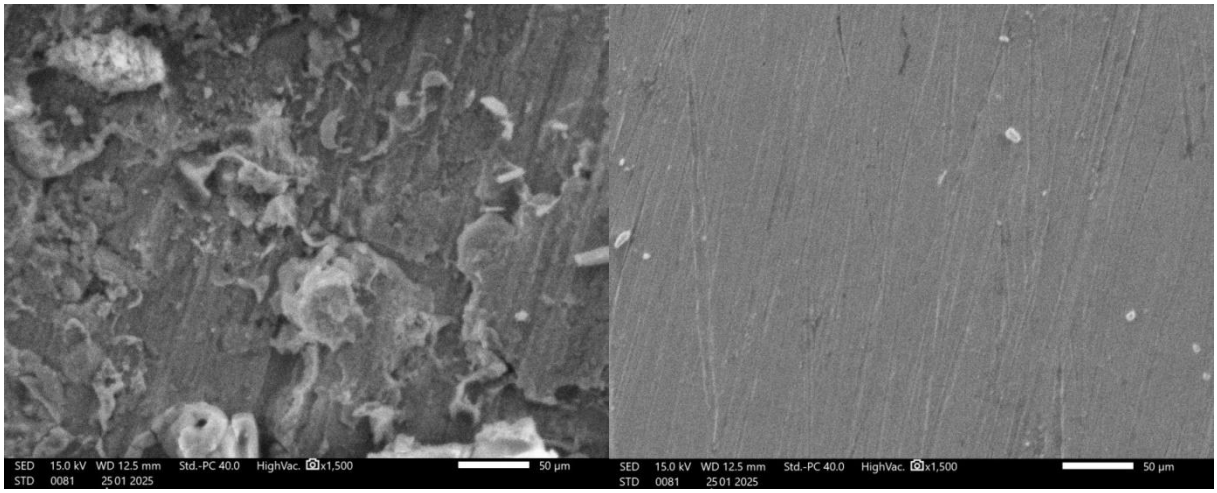

Figure (7): (a) SEM image for CS A283 in 2.0 M HCl solution. (b) SEM image for CS A283 in 2.0 M HCl solution in the presence of 500 ppm potato peel extract

3.6. Adsorption Isotherm

Potato peel extract inhibits the corrosion of CS A283 in 2.0 M HCl solution through adsorption onto the steel surface. This adsorption process is promoted by the exchange of water molecules previously adsorbed at the steel/solution interface. The mechanism can be described as an exchange mechanism, in which extract molecules from the aqueous phase, [Extract $_{(aq)}$] replaces *y* adsorbed water molecules, [$H_2O_{(s)}$] on the steel surface. As seen in the subsequent

equation, the displaced water molecules return to the bulk solution as [$H_2O_{(aq)}$] while the extract becomes adsorbed on the surface, [Extract $_{(s)}$].

$$\text{Extract}_{(aq)} + y\ H_2O_{(s)} \rightarrow \text{Extract}_{(s)} + y\ H_2O_{(aq)} \quad (6)$$

Where, **y** is the amount of adsorbed water molecules substituted by a one extract molecule.
The surface coverage values (θ) from PDP measurements were applied to multiple adsorption isotherm models to choose the most suitable adsorption isotherm for the adsorption process. The findings revealed that the adsorption of potato peel extract on the CS A283 surface obeyed the Langmuir adsorption isotherm. The applicability of this isotherm was confirmed by the excellent linear relationship obtained from the following Langmuir equation [48]:

$$\frac{C}{\theta} = \left(\frac{1}{K_{ads}}\right) + C \quad (7)$$

where, K_{ads} is the equilibrium constant of adsorption process

The standard free energy of adsorption $\Delta G°_{ads}$ is calculated using the equation [49]:

$$K_{ads} = \frac{1}{C_{H_2O}} exp\left(\frac{-\Delta G^0_{ads}}{RT}\right) \quad (8)$$

where, R is universal gas constant, C_{H_2O} is the concentration of water

The graphs between C/θ and C for the corrosion of CS A283 in a 2.0 M HCl solution with certain potato peel extract concentrations are presented in Fig8 . The resulting straight lines exhibited correlation coefficient (R^2) values close to unity, confirming that the adsorption of potato peel extract on the CS A283 surface obeys the Langmuir isotherm. The K_{ads} was determined from the intercept of these plots. This behavior is ascribed to the adsorbed inhibitor molecules forming a protective monolayer on the CS A283 surface with zero interaction between the adsorbed species. The estimated values of K_{ads} were identical to 0.09, whereas the determined values of ΔG_{ads} were -28.41 kJ mol^{-1}. The negative result demonstrates that a potato peel extract spontaneously adhered to the CS A283 surface. It is commonly known that values of ΔG_{ads} less than -20 kJ mol^{-1} propose physisorption, while values more than -40 kJ mol^{-1} imply chemical adsorption of the inhibitor on the metal surface [50]. This prove that the adsorption of potato peel extract on the CS A283 surface is physically. As an outcome, the measured ΔG_{ads} value indicates that physical adsorption predominates in the adsorption of potato peel extract on the CS A283 surface, with probable contributions from chemical adsorption.

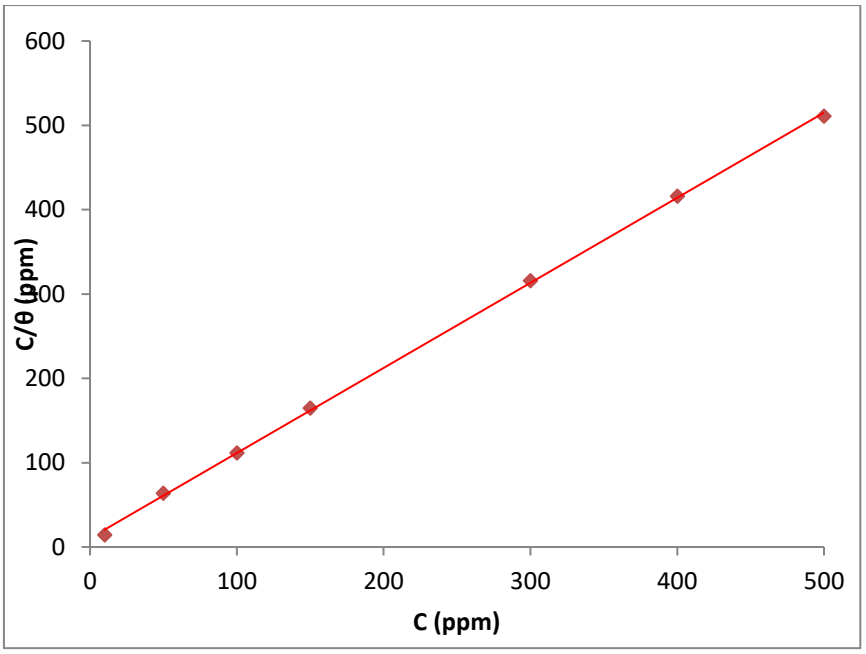

Figure (8): Langmuir isotherm for the adsorption of potato peel extract on CS A283 surface in 2.0 M HCl solution

3.7. **Computational Quantum and Monte Carlo Investigation of Potato Peel Bioactive Molecules**

Chemical reactions frequently take place in solutions, and determining the structures and energy of molecules in solutions is essential for predicting reaction mechanisms using DFT calculations. Since water remains the major component of the solvent system, even in 2.0 M HCl solution compared with 55.5 M H_2O, the effect of HCl concentration can be considered negligible. Therefore, the DFT calculations were performed in both aqueous medium and vacuum conditions for comparison.

Gaussian 09 gave us the quantum parameters of the optimized potato peel active molecules, to understand their reactivity in vacuum and in aqueous phase, **Tables 9-11**. With the help of χ_{Fe} = 4.06 eV and γ_{Fe} = 3.81 eV, and depending on energy of the highest occupied molecular orbital (E_{HOMO}), energy of the lowest occupied molecular orbital (E_{LUMO}), the ionization potential (I) or -E_{HOMO}, the electron affinity (A) or -E_{LUMO}, the given quantum parameters such as the absolute electronegativity (χ), the global hardness (γ) and the number of transferred electrons (ΔN) were calculated using the following equations [51]:

$$\Delta N = \frac{\chi_{Fe} - \chi_M}{2(\gamma_{Fe} + \gamma_M)} \quad (9)$$

$$\chi = \frac{(I+A)}{2} \quad (10)$$

$$\gamma = \frac{(I-A)}{2} \quad (11)$$

E_{HOMO} and E_{LUMO} respectively, convey information about donating and accepting electrons. Also, the difference between them (ΔE) indicates how reactive is the tested molecule, as lower (ΔE) indicates for more reactive is the optimized molecule.. The number of transferred electrons (ΔN) gives us information about electron accepting or electron donation; as in the case of $3.6 > \Delta N > 0$, the optimized molecule is more likely to donate electrons, while in the case of $\Delta N < 0$, the optimized molecule is more susceptible to accept electrons [52]. It is quite observable that the tested optimized molecules have ΔN more than zero and less than 3.6 (from 0.03 to 0.16) that these molecules can donate electrons to the empty d-orbitals on the steel surface. Furthermore, the EHOMO of these molecules is smaller than zero, implying that they can either receive electrons or physically adsorb on the Fe surface by electrostatic attraction[53].

Tables 9–11 display the amount of transferred electrons (ΔN) as follows:: α-Chaconine < Gallic acid < Caffeic acid < Quercetin < Chlorogenic acid < Petunidin. Also, the HOMO-LUMO gap (ΔE), the absolute electronegativity or the electron holding power (χ), and the global hardness or the electron cloud resistance against deformation under small electrical field perturbation (γ) are in the order: α-Chaconine > Gallic acid > Caffeic acid > Quercetin > Chlorogenic acid > Petunidin. This confirms that chlorogenic acid and petunidin have the highest ability for electron donation and hence highest adsorption tendency on steel surfaces, leading to more covering for metal surfaces and improved inhibition effectiveness [54, 55].

Figure 9 illustrates that the HOMO and LUMO densities of the five optimized potato peel molecules are distributed over the entire molecular structure, suggesting their ability to transfer electrons and form bonds with the steel surface .Furthermore, the regions of high electron density (red color) in the ESP maps are mainly concentrated around the O and N atoms, OH groups, C=O groups, and π-bonds, as expected.

Figure 10 presents the top and side views of the adsorbed potato peel molecules on the Fe (110) surface obtained from Monte Carlo simulation. The findings indicate that the adsorption of these compounds is more favorable than that of the corrosive medium. The optimized molecules tend to migrate toward the steel/interface region and adopt a nearly horizontal orientation, leading to

maximum surface coverage of the Fe surface. The calculated adsorption energies listed in Table 11 range from −77.48 to −353.59 kcal/mol. These extremely negative values attest the spontaneous adsorption of the active potato peel molecules on the CS A283 surface via a combination of chemical and physical interactions.

	ESP	HOMO and LUMO
α-chaconine	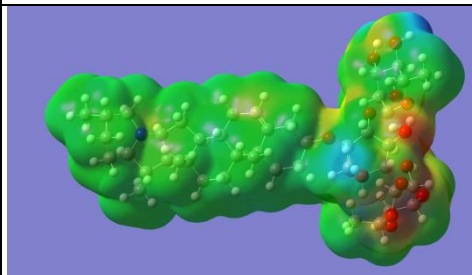	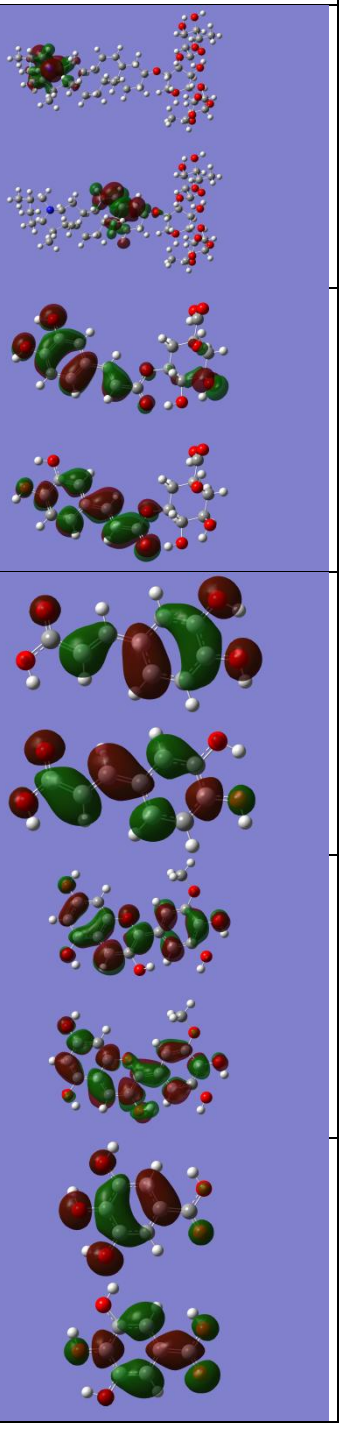
Chlorogenic acid	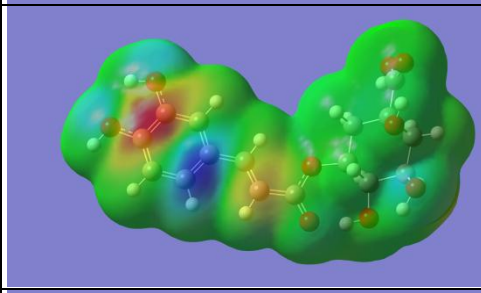	
Caffeic acid	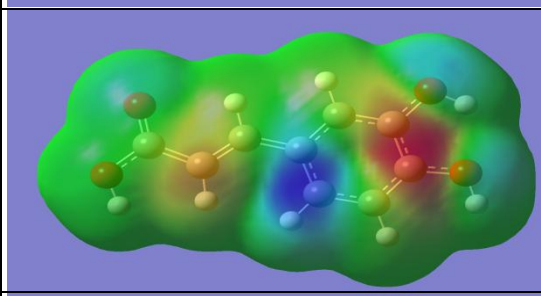	
Petunidin	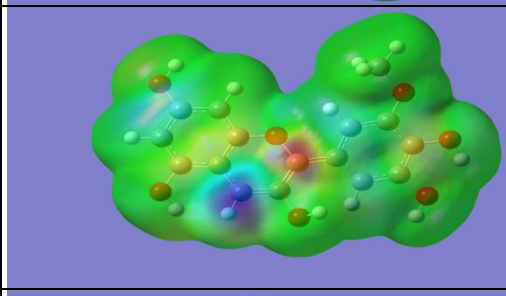	
Gallic acid	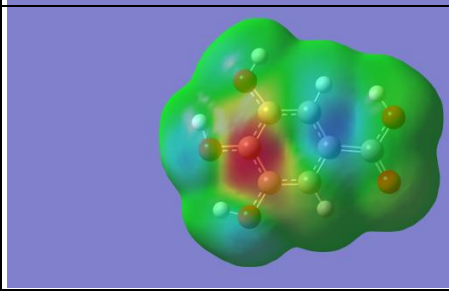	

The

	ESP	HOMO and LUMO
Quercetin	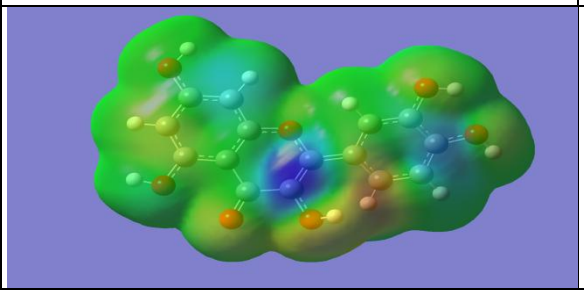	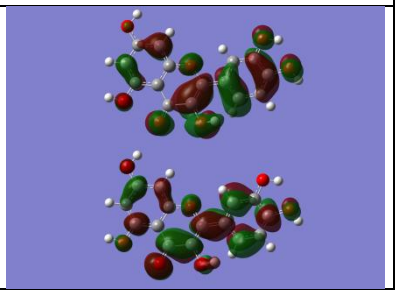

Figure (9): ESP, HOMO and LUMO of the potato peel bioactive compounds

	Side and top Simulation views
α-chaconine	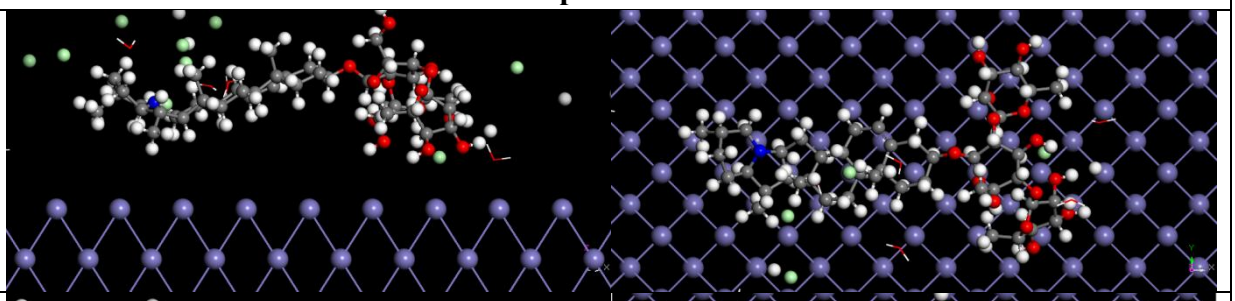
Chlorogenic acid	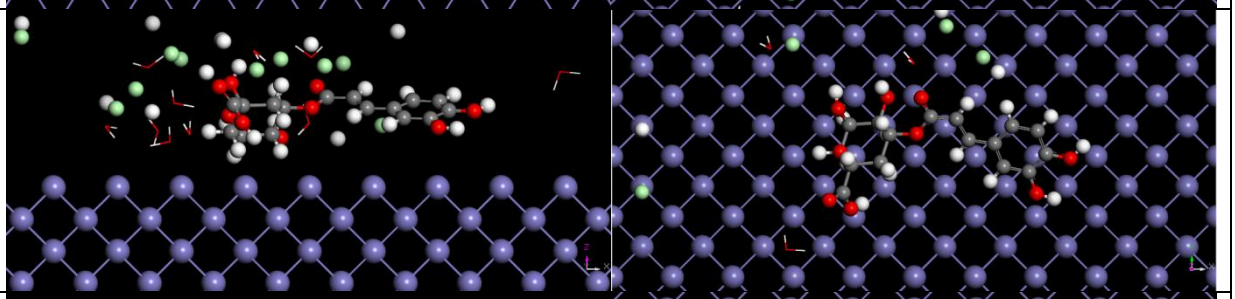
Caffeic acid	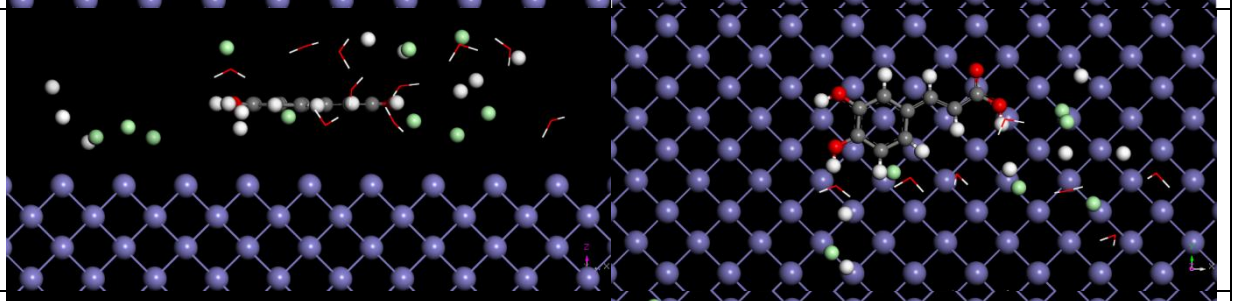
Petunidin	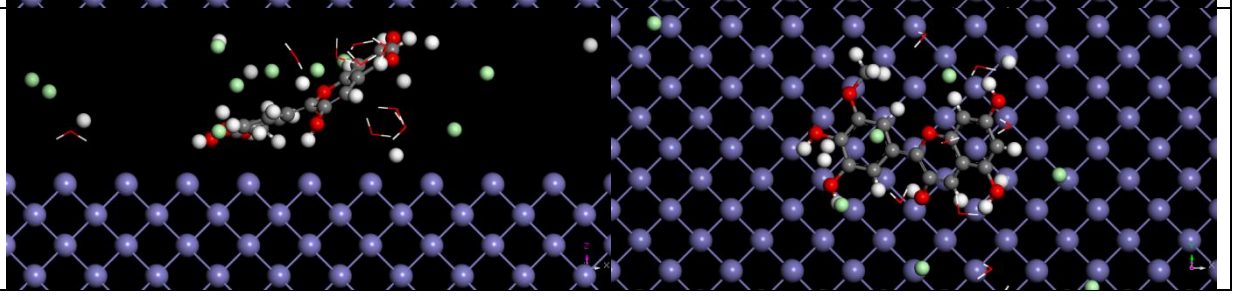

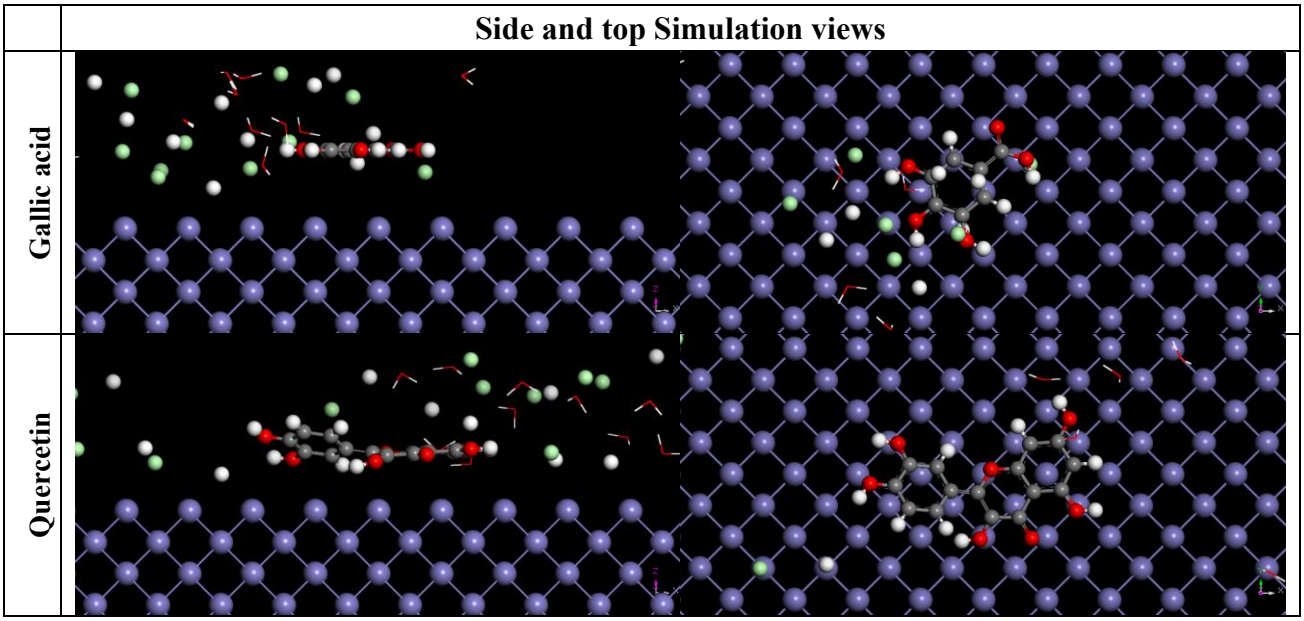

Figure (10): Monte Carlo simulation of the potato peel bioactive compounds

Table (9): Vacuum quantum parameters of potato peel optimized molecules

Parameters	α-Chaconine	Gallic acid	Caffeic acid	Quercetin	Chlorogenic acid	Petunidin
E_{HOMO} (eV)	-5.91	-5.01	-4.82	-4.44	-4.20	-3.85
E_{LUMO} (eV)	0.70	-0.60	-0.62	-0.79	-0.80	-0.80
ΔE (eV)	6.61	4.41	4.19	3.65	3.39	3.05
I (eV)	5.91	5.01	4.82	4.44	4.20	3.85
A (eV)	-0.70	0.60	0.62	0.79	0.80	0.80
χ (eV)	2.61	2.81	2.72	2.61	2.50	2.32
γ (eV)	3.31	2.21	2.10	1.82	1.70	1.53
ΔN (e)	0.10	0.10	0.11	0.13	0.14	0.16

Table (10): Aqueous phase quantum parameters of potato peel optimized molecules

Parameters	α-Chaconine	Gallic acid	Caffeic acid	Quercetin	Chlorogenic acid	Petunidin
E_{HOMO} (eV)	-8.82	-6.00	-5.52	-5.27	-4.79	-3.97
E_{LUMO} (eV)	1.61	-1.23	-1.33	-1.53	-1.43	-0.69
ΔE (eV)	10.43	4.78	4.19	3.75	3.36	3.28
I (eV)	8.82	6.00	5.52	5.27	4.79	3.97
A (eV)	-1.61	1.23	1.33	1.53	1.43	0.69
χ (eV)	3.61	3.62	3.43	3.40	3.11	2.33
γ (eV)	5.21	2.39	2.10	1.87	1.68	1.64
ΔN (e)	0.03	0.04	0.05	0.06	0.09	0.16

Table (11): Monte Carlo measurements of adsorption simulation of potato peel optimized molecules on Fe (110)

Energy (kcal/mol)	α-Chaconine	Gallic acid	Caffeic acid	Quercetin	Chlorogenic acid	Petunidin
E_{ads}	-77.48	-111.46	-119.81	-152.90	-291.84	-353.59
dE_{ads}/dN_{H2O}	-1.89	-1.91	-1.77	-1.84	-1.55	-1.84
dE_{ads}/dN_{HCl}	-0.60	-0.50	-0.52	-0.45	-0.26	-0.46
dE_{ads}/dN_{i}	-50.44	-84.07	-93.30	-126.84	-272.10	-327.65

In conclusion, due to their substantial adsorption onto the surface of steel, the optimized main bioactive compounds found in potato peel show considerable promise as corrosion inhibitors. This adsorption process is facilitated by the transfer of electrons from the heteroatoms and π-electron systems of the molecules to the vacant d-orbitals of the iron surface, in addition to the electrostatic pull between the polarized inhibitor molecules and the charged steel surface. The combination of physical and chemical interactions create a compact and stable protective adsorbed layer that successfully isolates the steel surface from the aggressive corrosive media and suppresses the rate of corrosion. The excellent inhibitory performance of potato peel extract is confirmed by the theoretical results derived from DFT and Monte Carlo simulations, which accord well with the experimental findings.

3.8.Mechanism of inhibition

Potato peel extract was investigated as a green corrosion inhibitor for CS A283 in a 2.0 M HCl solution. The extract substantially minimizes the rate of corrosion, according to results from both chemical and electrochemical measurements. The inhibitory impact is mainly caused by the adsorbing of extract's components to the steel surface, creating a barrier that hinders the steel dissolution and suppresses electrochemical processes at the interface. The inhibitory mechanism is controlled by the interaction between the adsorbed molecules and the CS A283 surface, which is influenced by factors such as surface coverage, molecular structure, and electron-donating capacity. The extract contains several bioactive compounds, including -chaconine, chlorogenic acid, caffeic acid, petunidin, gallic acid, and quercetin. Numerous functional groups, such as hydroxyl and aromatic rings, improve these molecules' attraction for the steel surface and provide multiple adsorption sites [56]. Consequently, these components tend to adsorb primarily in a parallel orientation, which maximizes surface coverage and results in the creation of a compact and stable protective layer. This protective layer improves corrosion resistance by

effectively separating the steel from the corrosive acidic medium.The inhibitory process was mostly accomplished through physical adsorption via electrostatic interactions between the potato peel extract molecules and the steel surface, according to both the experimental findings and quantum chemical predictions

The mechanism of physisorption includes the creation of a protective film on the CS A283 surface through weak electrostatic interactions between the potato peel molecules and the charged steel surface. Unlike chemisorption, this process is generally rapid, reversible, and strongly influenced by temperature. The adsorbed potato peel molecules act as a physical barrier that blocks the active sites responsible for the anodic and cathodic corrosion reactions. The adsorption energy is typically lower than −40 kJ mol^{-1}, indicating relatively weak interactions between the potato peel molecules and the steel surface. As the temperature increases, the kinetic energy of the adsorbed species also increases, promoting desorption of the potato peel molecules and consequently reducing the inhibition efficiency. Moreover, because physisorption is reversible, a decrease in potato peel extract concentration in the corrosive HCl solutions may lead to partial or complete removal of the protective layer. In contrast to chemisorption, which commonly forms a stable monolayer, physisorption may allow the formation of multilayer adsorption on the metal surface [57].

Polarized potato peel molecules or protonated species are electrostatically attracted to the charged steel surface. These adsorbed molecules are stabilized by weak intermolecular van der Waals forces on the steel surface. As the potato peel molecules eventually replace the water molecules that were initially adsorbed at the steel/solution interface, a protective adsorbed layer develops.This layer obstructing both anodic and cathodic active sites, thereby reducing the corrosion current and suppressing the corrosion process. The adsorption process occurs spontaneously as the system tends to attain a lower energy state through adsorption at the HCl/steel interface, resulting in a decrease in ΔG_{ads}, typically around −20 kJ mol^{-1}, which is characteristic of physical adsorption [58].CS A283 is is highly reactive in HCl solution. The existence of carbon and surface heterogeneities create active sites that accelerate the corrosion process. Cl ions from the acid are smaller and more mobile than the bulky potato peel molecules, allowing them to rapidly approach and adsorb onto the steel surface. These chloride ions interact with the vacant 3d orbitals of iron atoms, producing an excess negative charge at the steel /solution interface.

In acidic media, the potato peel molecules become protonated after accepting H^+ ions from the solution. The positively charged protonated species are then electrostatically attracted to the negatively charged surface already enriched with adsorbed chloride ions. Consequently, adsorption occurs mainly through physical adsorption, where electrostatic interactions stabilize the inhibitor layer on the steel surface. This adsorbed protective film blocks both anodic and cathodic active sites, thereby reducing the corrosion rate.Once the inhibitor molecules approach the CS A283 surface, their nucleophilic centers can displace previously adsorbed water or acid molecules and form a more stable adsorbed layer on the metal. In addition, some vacant 3d orbitals of iron atoms generate positively charged or electrophilic centers on the steel surface, which promote the attraction of polarized inhibitor molecules. Even in the absence of strong chemical bond formation, these vacant orbitals facilitate dipole–dipole interactions between the potato peel molecules and the metal surface, allowing the molecules to remain adsorbed on the steel through physical interactions. The active constituents of Potato Peel extract contain aromatic benzene rings, π-electron systems, and lone-pair electrons on oxygen atoms. These structural features increase the electron density and adsorption tendency of the molecules. Therefore, the inhibitor molecules adsorb strongly onto the electrophilic sites at the steel/solution contact, lowering the overall energy of the system and enhancing the corrosion protection efficiency.

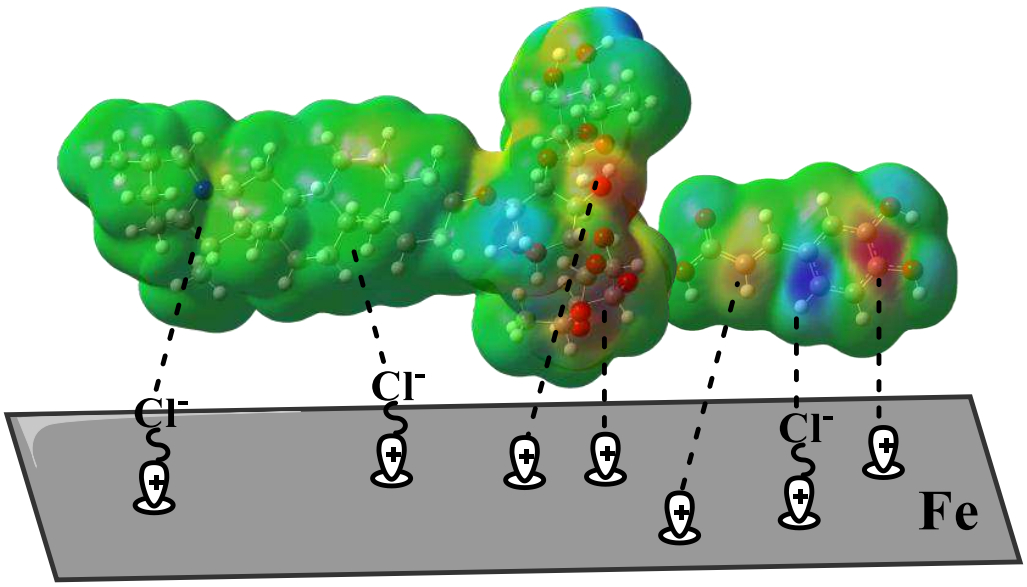

Figure (11): Adsorption of polarized potato peel molecules onto the empty and the chloride-covered 3d orbitals of the CS A283 surface

Conclusion

Potato peel was successfully extracted using alcohol, and the structure of its bioactive components was confirmed by mass spectroscopy, FT-IR, ^{1}H NMR, and ^{13}C NMR investigations. Using chemical and electrochemical methods, the potato peel extract was evaluated as a corrosion inhibitor for CS A283 in a 2.0 M HCl solution. The outcomes demonstrated that the extract had good corrosion prevention performance. At lower temperatures and with increasing extract concentration, the inhibition efficiency increases. The extract's spontaneous adsorption onto the CS A283 surface is responsible for its inhibitory effectiveness. It was discovered that the Langmuir adsorption isotherm governed the adsorption process. According to the DFT computation, petunidin and chlorogenic acid have the highest electron-donating capacity and, as a result, the greatest propensity for adsorption onto the steel surface, leading to superior corrosion inhibition efficiency.

Data availability

The datasets used and analyzed during the current study are available from the corresponding author on reasonable request.

References

1. Krid,F., Zouaoui, F. E. , Medjram, M.S., Aqueous extracts of Opuntia Ficus-Indica as green corrosion inhibitor of A283C carbon steel IN 1N sulfuric acid solution, Chem. Chem. Technol., 12 ,405-409. https://doi.org/10.23939/chcht12.03.405(2018)
2. Zheng, B. Zhang, X. Wang, Y. Lu, F. Li, C. Li. Improved corrosion resistance of carbon steel in soft water with dendritic-polymer corrosion inhibitors. Chem Eng J 452,139043. https://10.1016/j.cej.2022.139043 (2023) .
3. Tan B., et al. Insight into anti-corrosion nature of Betel leaves water extracts as the novel and eco-friendly inhibitors. J Colloid Interface Sci .585, 287. https://10.1016/j.jcis.2020.11.059. (2021)
4. Sarkar T.K.,Mechanistic evaluation of adsorption and corrosion inhibition capabilities of novel indoline compounds for oil well/tubing steel in 15% HCl. Chem. Eng. J. 431:133481. https://10.1016/j.cej.2021.133481(2022)
5. Abdulhadi Kadhum, et.al., Corrosion inhibitors. A review. Int. J. Corros. Scale Inhibition. 10(1), 54-67.DOI: 10.17675/2305-6894-2021-10-1-3. (2011).
6. Haque, J., Ansari, K. R., Srivastava, V., Quraishi, M. A. & Obot, I. B. Pyrimidine derivatives as novel acidizing corrosion inhibitors for N80 steel useful for petroleum

industry: A combined experimental and theoretical approach. *J. Ind. Eng. Chem.* **49**, 176–188. https://doi.org/10.1016/j.jiec.2017.01.025 (2017)
7. Barrahi, A. et.al. Adsorption and inhibition mechanism of pyrazole derivatives on carbon steel: Combined electrochemical, surface, and DFT/MD study, *RSC Advances,* 16,15531, DOI: 10.1039/d6ra00508j. (2026)
8. Thami Laabaissi, et.al. Experimental and molecular modeling approach on the corrosion behavior of mild steel in HCl solution with quinoxaline inhibitors, J. Dispersion Science and Technology , 47(3), 549–562 https://doi.org/10.1080/01932691.2024.2417682. (2026)
9. Belkheiri, A. et al. In-depth study of a newly synthesized imidazole derivative as an eco-friendly corrosion inhibitor for mild steel in 1 M HCl: Theoretical, electrochemical, and surface analysis perspectives. *Int. J. Electrochem. Sci.* **19**, 100768 .https://doi.org/10.1016/j.ijoes.2024.100768. (2024).
10. Metwally Abdallah .et.al. Assessment *of* poly (4-vinyl pyridine), polyvinylpyrrolidone compounds as prospective corrosion inhibitors for low carbon steel in sulfuric acid: Experimental and theoretical approaches, *J. Disper. Sci. and Tech.*, 47(4), 679–695 DOI: 10.1080/01932691.2024.2420887. (2026).
11. Zhang, Q. H. et al. Comparison of the synergistic inhibition mechanism of two eco-friendly amino acids combined corrosion inhibitors for carbon steel pipelines in oil and gas production. *Appl. Surf. Sci.* **583** https://doi.org/10.1016/j.apsusc.2022.152559 (2022)
12. Mahmoud G. A. Saleh. et.al., Original hydrazine carbothioamide Schiff base derivative as a suitable mitigator for corrosion of carbon steel and hydrogen production in acidic aqueous media, *J .Electrochem. Sci. and Eng.,* 15 (5) 2546 DOI: https://doi.org/10.5599/jese.2546. (2025).
13. Majda Alfakeer, et.al. Synthesis and Cyclic Voltammetric Studies of Azo Dye Compounds Derived from 1,5-Dihydroxynaphthalene and Their Application as Corrosion Inhibitors for Carbon Steel in Hydrochloric Acid Solution, *Int. J. Electrochem. Sci.* **,** 20 (1), 100892, https://doi.org/10.1016/j.ijoes.2024.100892. (2025).
14. Metwally Abdallah, et.al. Experimental and theoretical insights into the inhibitory capabilities of polythiophene and polypyrrole molecules for protecting mild steel from corrosion in sulfuric acid, *Scientific Reports*,16 ,15045, https://doi.org/10.1038/s41598-026-50293-9 . (2026).
15. Mohamed I. Ahmed, et.al. Corrosion inhibition mechanism of a functionalized schiff base–derived quaternary ammonium salt for carbon steel in 1 M HCl: electrochemical, adsorption, and theoretical studies.*Scientific Reports* **16**, 11618 .https://doi.org/10.1038/s41598-026-41236-5.(2026).
16. Khamis,et.al., Eco-friendly inhibitors for sustainable corrosion protection of mild steel under oilfield acidizing conditions *Scientific Reports* **. 15**, Article number: 42549 https://doi.org/10.1038/s41598-025-27271-8 ,(2025).
17. Rahmouni, H. et al. ,Experimental and theoretical investigations into green approach steel corrosion Inhibition performance of an aqueous mixture of Olea Europaea and ficus carica leaves extract in acid medium. *Royal Soc. Chem. Adv.* **15** (26), 20355–20371. https://doi.org/10.1039/D5RA02786A (2025).
18. Chen, S. et al. ,Solanum tuberosum leaf extract as an eco-friendly corrosion inhibitor for Q235-steel in HCl medium: experimental and theoretical evaluation. *Int. J. Electrochem. Sci.* **19** (Issue 11), 100818. https://doi.org/10.1016/j.ijoes.2024.100818 (2024).

19. Aldahiri, R. H., Hussein, M. A. & Al-Bukhari, S. M. A. Synergistic effect of canarium strictum leaves extract and KI on the corrosion protection of mild steel in 15% HCl solution. *Sci. Rep.* **15**, 3576. https://doi.org/10.1038/s41598-025-87482-x (2025)
20. Kumar, A. & Das, C. ,A novel eco-friendly inhibitor of chayote fruit extract for mild steel corrosion in 1 M HCl: Electrochemical, weight loss studies, and the effect of temperature. *Sustainable Chem.Pharm.* **36**,101261. https://doi.org/10.1016/j.scp.2023.101261 (2023).
21. Abdel Hameed, R. S. et.al., Spinacia oleracea Extract as green corrosion inhibitor for carbon steel in hydrochloric acid solution, *Int. J. Electrochem. Sci.,* 17, 221017, doi: 10.20964/2022.10.31 (2022).
22. Metwally Abdallah, et. al. Exploring Cinnamon Extract's Potential as a Green Corrosion Inhibitor for X65 Carbon Steel in Sulfuric Acid: A Comprehensive Investigation, *J. Disper. Sci. and Tech.*,,46(9) 1475-1489 https://doi.org/10.1080/01932691.2024.2333537 (2025)
23. El-Etre. et.al. Corrosion Inhibition of Some Metals Using Lawasonia Extract , *Corros. Sci.,*47(2), (2005)385-395 . https://doi.org/10.1016/j.corsci.2004.06.006.
24. Abdallah, M. et.al.,Some natural aqueous extracts of plants as green inhibitor for dissolution of carbon steel in 0.5M sulfuric acid, *Green Chem. Lett.Rev*.2018,11(3)189-196 ,DOI: 10.1080/17518253.2018.1458161
25. Metwally Abdallah, et. al. Insights into the effectiveness of natural Mentha oil in mitigating the corrosion of carbon steel in sulfuric acid, *Green Chem. Lett.Rev*.,18 NO. 1 (2025) 2527724 **.** https://doi.org/10.1080/17518253.2025.2527724
26. Metwally Abdallah et.al., on the corrosion of mild steel in sulfuric acid solution: Chemical, electrochemical, computational aspects, *Green Chem. Lett.Rev*.,16(11) (2023) 2249019doi.org/10.1080/17518253.2023.2249019.
27. Abdallah, M. et.al. Natural nutmeg oil as a green corrosion inhibitor for carbon steel in 1.0 M HCl solution: Chemical ,electrochemical and computational methods, *J. Mol. Liq., ,*323(2021)115036., https://doi.org/10.1016/j.jtice.2019.12.006
28. O. Awogbemi, D.V.V. Kallon, A.O. Owoputi, Biofuel generation from potato peel waste: current state and prospects, Recycling, 7 ,23. DOI: 10.3390/recycling7020023 (2022).
29. Jimenez-Champi, D. et.al.,Bioactive compounds in potato peels, extraction methods, and their applications in the food industry: a review, Cyta-journal of Food, 21, 418-432. DOI: 10.1080/19476337.2023.2213746 (2023).
30. Sampaio.S.L., Potato peels as sources of functional compounds for the food industry: A review, Trends in Food Science & Technology, 103 ,118-129 DOI: 10.1016/j.tifs.2020.07.015 (2020).
31. Mathur, P.; Vasudevan, T. Reaction rate studies for the corrosion of metals in acids—I, iron in mineral acids. *Corrosion*. **38**, 171-178. doi: 10.5006/1.3579270. (1982).
32. P.D. Pathak, S.A., Valorization of potato peel: a biorefinery approach, Critical Reviews in Biotechnology, 38 (2018) 218-230. DOI: 10.1080/07388551.2017.1331337
33. Abdallah, M. et.al., Sildenafil drug as a safe anticorrosion for 6063 aluminum alloy in acidic and alkaline solutions: Theoretical and experimental studies, Egypt. *J. Pet*., **29**(3) 211-218. https://doi.org/10.1016/j.ejpe.2020.06.001. (2020).

34. Daoudi,W.et.al. Essential oil of Dysphania ambrosioides as a green corrosion inhibitor for mild steel in HCl solution, J. Mol. Liquids, 363 ,119839. https://doi.org/10.1016/j.molliq.2022.119839 (2022).
35. Rasha N. Felaly, et.al.,Experimental and computational evaluation of expired anticonvulsant drugs as corrosion inhibitors for 316 stainless steel in HCl solutions **,**Int. J. Electrochem.Sci.,21(2), 101264 https://doi.org/10.1016/j.ijoes.2025.101264. (2026).
36. Metwally Abdallah.et.al., Experimental and theoretical insights into the inhibitory capabilities of polythiophene and polypyrrole molecules for protecting mild steel from corrosion in sulfuric acid, *Scientific Reports*,16 ,15045, https://doi.org/10.1038/s41598-026-50293-9 . (2026)
37. Sobhi. M. Gatifloxacin as Corrosion Inhibitor for Carbon Steel in Hydrochloric Acid Solutions, Protec.Metals and Phys. Chem of Surf. 50 (6), 825-832. DOI: 10.1134/S2070205114060227(2014).
38. Elsaoud A.A.et.al. Recyclization of expired Megavit Zinc (MZ) drug as metallic corrosion inhibitor for copper alloy C10100 in nitric acid solution, J. Bio-and Tribo-Corros., 7 ,1-9. DOI: 10.1007/s40735-021-00494-8(2021).
39. Verma C. et.al.,Principles and theories of green chemistry for corrosion science and engineering: design and application, Green Chemistry, 26 ,4270-4357. DOI: 10.1039/D3GC05207A. (2024).
40. Metwally Abdallah et.al. Assessment of quinazoline derivatives as efficient corrosion inhibitor for carbon steel in acidic environment. A theoretical and practical analysis, Int. J. Electrochem. Sci. 20 .100990 , https://doi.org/10.1016/j.ijoes.2025.100990. (2025).
41. A.H. Tantawy, K.A. Soliman, H.M. Abd El-Lateef, Novel synthesized cationic surfactants based on natural piper nigrum as sustainable-green inhibitors for steel pipeline corrosion in CO2-3.5% NaCl: DFT, Monte Carlo simulations and experimental approaches, Journal of Cleaner Production, 250, 119510. https://doi.org/10.1016/j.jclepro.2019.119510. (2020).
42. Arej S. Al-Gorair. et.al. Assessments of Licorice Root Extract as an Environmentally Benign Corrosion Inhibitor for Aluminum in HCl Solutions , *Int. J. Electrochem. Sci.,* 21(2), 101343.https://doi.org/10.1016/j.ijoes.2026.101343. (2026)
43. Laider, K.J. , Chemical Kinetics, Mc Graw Hill Publishing Company Ltd, New York,(1965).
44. Riggs Jr, O. L., Hurd, R. M., Temperature coefficient of corrosion inhibition, *Corrosion, ,***23(**8) , 252-258. DOI: 10.5006/0010-9312-23.8.252. .(1967).
45. D.F. Seyam, S. Eid, A.H. Tantawy, Study the Inhibition effect of Three Newly Synthesized Schiff Base Based Cationic Surfactants on Aluminum Corrosion in 0.5 M HCl Solution, Egypt. J. Chem, 66 ,87-99 . DOI:10.21608/EJCHEM.2022.134981.5942 (2023).
46. Muthukrishnan P., Stigmasterol extracted from Ficus hispida leaves as a green inhibitor for the mild steel corrosion in 1 M HCl solution, Arabian Journal of Chemistry, 12 ,3345-3356. DOI:10.1016/j.arabjc.2015.09.005 (2019).
47. Verma et.al., Principles and theories of green chemistry for corrosion science and engineering: design and application, Green Chemistry, 26 ,4270-4357. https://doi.org/10.1039/D3GC05207A (2024).
48. A.A. Elsaoud, E.M. Mabrouk, D.F. Seyam, A. El-Etre, Recyclization of expired Megavit Zinc (MZ) drug as metallic corrosion inhibitor for copper alloy C10100 in

nitric acid solution, Journal of Bio-and Tribo-Corrosion, 7 ,1-9. DOI:10.1007/s40735-021-00494-8 (2021).
49. kosari. A. et.al., Electrochemical and quantum chemical assessment of two organic compounds from pyridine derivatives as corrosion inhibitors for mild steel in HCl solution under stagnant condition and hydrodynamic flow. Corros.Sci., 78, 138-150 . https://doi.org/10.1016/j.corsci.2013.09.009 (2014).
50. Pearson, R.G. Absolute electronegativity and hardness: application to inorganic chemistry, Inorganic chemistry, 27,734-740. http://dx.doi.org/10.1021/ic00277a030 (1988).
51. Pour-Ali, S. , Hejazi, S., Tiazofurin drug as a new and non-toxic corrosion inhibitor for mild steel in HCl solution: Experimental and quantum chemical investigations, *J. Mol. Liq.,*, 354, 118886. DOI:10.1016/j.molliq.2022.118886 (2022).
52. Abdallah, M. et.al. Insights into corrosion inhibition of aluminum in hydrochloric acid solutions using expired cephalosporins and klavox: Chemical, electrochemical and theoretical approaches. *Int. J. Electrochem. Sci.,* 19 ,100741. https://doi.org/10.1016/j.ijoes.2024.100741(2024)
53. Ghosh D.C., Islam N. Whether electronegativity and hardness are manifest two different descriptors of the one and the same fundamental property of atoms—A quest, International Journal of Quantum Chemistry, 111 ,40-51. DOI: 10.1002/qua.22415. (2011).
54. Islam N., Ghosh. D.C. Evaluation of global hardness of atoms based on the commonality in the basic philosophy of the origin and the operational significance of the electronegativity and the hardness. Part I. The Gordy's scale of electronegativity and the GH, European Journal of Chemistry, 1 83-89. DOI: 10.5155/eurjchem.1.2.83-89.26 (2010).
55. Anderson J.S., Melin J. ,Ayers, P.W. Conceptual density-functional theory for general chemical reactions, including those that are neither charge-nor frontier-orbital-controlled. 1. Theory and derivation of a general-purpose reactivity indicator, Journal of Chemical Theory and Computation, 3 ,358-374. DOI: 10.1021/ct600164j (2007).
56. Othman, K.A. Hamad. W.M, Omer. R.A. Theoretical and experimental exploration of organic molecules adsorption on iron surfaces for corrosion inhibition: a review, Corrosion Reviews, 43 ,335-359. DOI: 10.1515/corrrev-2024-0039 (2025).
57. Kokalj .A. Corrosion inhibitors: physisorbed or chemisorbed?, Corrosion Science, 196 ,109939. DOI: 10.1016/j.corsci.2021.109939 (2022).
58. Shalabi et.al. Green synthesizing and corrosion inhibition characteristics of azo compounds on carbon steel under sweet conditions: experimental and theoretical approaches, ACS omega, 9 18932-18945. https://doi.org/10.1021/acsomega.3c09072 (2024).